Available online at www.sciencedirect.com

ScienceDirect

Tectonophysics 464 (2009) 164 – 185

TECTONOPHYSICS

www.elsevier.com/locate/tecto

Eocene adakitic volcanism in southern British Columbia: Remelting of arc basalt above a slab window

Ryan B. Ickert [a,*,1], Derek J. Thorkelson [a], Daniel D. Marshall [a], Thomas D. Ullrich [b]

[a] *Department of Earth Sciences, Simon Fraser University, Burnaby, British Columbia, Canada V5A 1S6*
[b] *Pacific Centre for Isotopic and Geochemical Research, Earth and Ocean Sciences, University of British Columbia, Vancouver, British Columbia, Canada V6T 1Z4*

Received 13 April 2007; received in revised form 8 October 2007; accepted 31 October 2007
Available online 6 November 2007

Abstract

The Princeton Group is an assemblage of terrestrial volcanic and clastic sedimentary rocks in south-central British Columbia, and is part of the Challis–Kamloops belt that stretches from central British Columbia to the northwestern United States. The volcanic rocks were largely deposited as cinder cones and composite volcanoes, and are composed of basaltic andesite (olivine + clinopyroxene), andesite and dacite (hornblende + plagioclase + clinopyroxene), and rhyolite (biotite + quartz + K-feldspar), with calc–alkaline affinity. New ^{40}Ar/^{39}Ar dates on hornblende and groundmass separates, and whole rock indicate that magmatism took place during the Early to Middle Eocene, from 53–47 Ma. New neodymium isotopic measurements, in conjunction with previously published results, indicate that the Princeton Group has an $\varepsilon\mathrm{Nd}_{50} = 1.2–6.4$ and therefore represents primarily juvenile additions to the continental crust.

The major and trace element abundances of Princeton Group rocks resemble those of many modern continental arcs. The compositions are notable, however, because they have an "adakitic" signature that extends throughout their entire compositional range, including high-Mg# basaltic andesite. Trace element modelling indicates that this signature was not derived from anatexis of normal oceanic crust, but from an "arc-like" source enriched in large-ion lithophile elements. This source may have been basaltic dykes that were emplaced into the lithospheric mantle during Mesozoic arc magmatism and subsequently partially melted during an event of lithospheric heating in the Eocene. The heating may have been caused by upwelling asthenosphere related to a slab window or slab tear.

Keywords: Adakite; Slab window; Volcanism; Eocene; Geochemistry; British Columbia

1. Introduction

The Princeton Group represents part of an intense, early Tertiary magmatic event that affected large areas of western North America (Fig. 1). In the interior of southern British Columbia and the northwestern United States, the magmatic event is preserved mainly as volcanic successions of the Challis–Kamloops belt (Souther, 1991). This belt stretches ~1500 km from central BC, where it is 200 km wide, into Idaho and Wyoming where it broadens to over 500 km. Although the separate volcanic fields of the Challis–Kamloops belt have been the focus of numerous studies (Ewing, 1981a,b; Dudas, 1991; Norman and Mertzman, 1991; McKervey, 1998; Morris et al., 2000; Dostal et al., 2001; Breitsprecher, 2002; Feeley et al., 2002; Dostal et al., 2003; Feeley, 2003; Feeley and Cosca, 2003; Lindsay and Feeley, 2003; Morris and Creaser, 2003), consensus has not been reached on the relationship of igneous activity to plate tectonics (cf. Breitsprecher et al., 2003; Feeley, 2003). Workers in different parts of the Challis–Kamloops belt have attributed volcanic activity to a variety of mechanisms including typical arc volcanism (Ewing, 1980; Morris and Creaser, 2003), rifting in a volcanic arc (Dostal et al., 2001, 2005), decompression melting (Dudas, 1991; Norman and Mertzman, 1991; Morris and Hooper, 1997; Morris et al., 2000), and arc to intraplate processes related to a slab window (Thorkelson and Taylor, 1989; Breitsprecher et al., 2003; Dostal et al., 2003; Haeussler et al., 2003). The differences in

---

[*] Corresponding author. Fax: +1 61 02 6125 8345.
E-mail address: Ryan.Ickert@ualberta.net (R.B. Ickert).

[1] Currently at: Research School of Earth Sciences, Australian National University, Canberra, A.C.T. 0200, Australia.

0040-1951/$ - see front matter © 2007 Elsevier B.V. All rights reserved.
doi:10.1016/j.tecto.2007.10.007

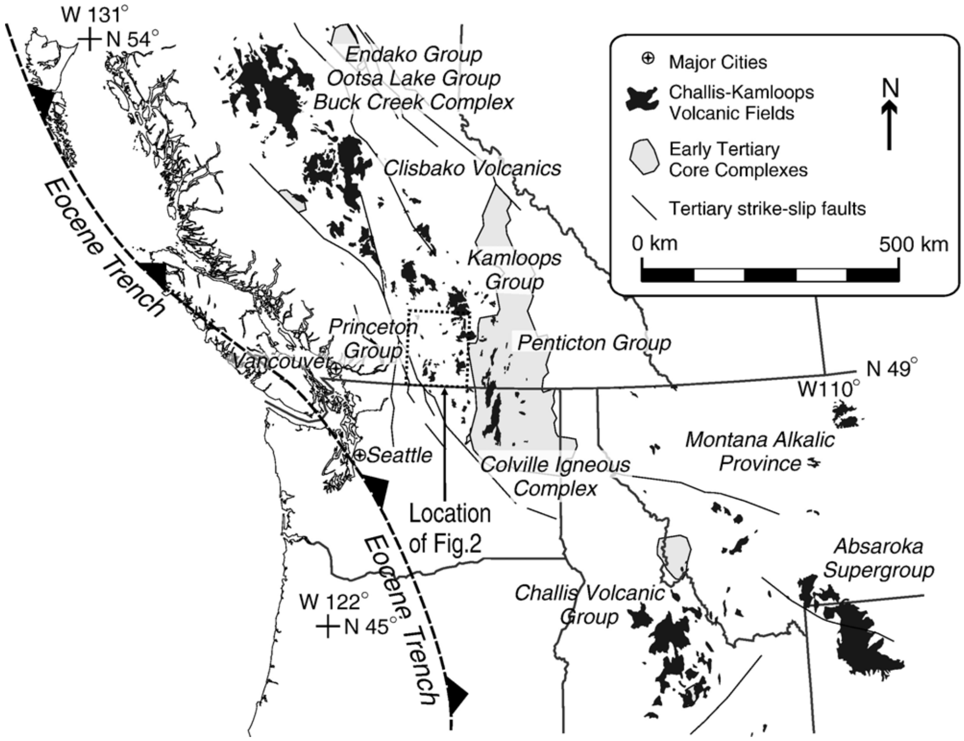

Fig. 1. Map of Eocene volcanic fields in the Challis–Kamloops Belt and related geological features. After Burchfiel (1993), Dickinson (1991), Wheeler and McFeeley (1991), and Breitsprecher (2002).

interpreted tectonic setting commonly diverge near the United States–Canada border, with arc processes commonly appealed to in the north, and intraplate processes typically invoked to the south.

The presence of adakites (Defant and Drummond, 1990) and adakitic high-Mg# andesites (Kelemen et al., 2003; Mg# = molar $100 \times \mathrm{Mg}/[\mathrm{Mg}+\mathrm{Fe}^{2+}]$) in the Princeton Group raises important questions about the geodynamic setting of Southern BC during the Eocene (Breitsprecher et al., 2003). Adakites are an important class of intermediate to silicic composition lavas with high Sr/Y and La/Yb that are most often associated with partial melting of garnet-bearing metabasalt, in particular the partial melting off young, subducted oceanic crust. High-Mg# andesites are commonly associated with adakites (and sometimes Nb-enriched basalts) and have similar trace element signatures, but are much more mafic. Controversy surrounds the interpretation of adakites (Garrison and Davidson, 2003), as the geochemical signature is not unique to a single process or tectonic setting (Atherton and Petford, 1993; Feeley and Hacker, 1995; Xu et al., 2002). Volcanic rocks in the Princeton Group have an adakitic geochemical signature present over a wide range of bulk compositions, from highly evolved rhyolite to primitive basaltic andesite. Evolved ($SiO_2 > 63$ wt.%, Mg# < 45) adakites are typically interpreted as melts of lower continental crust that have not interacted with peridotite, whereas primitive (mafic) adakites are often inferred to have traversed the mantle wedge after genesis by partial melting of subducted crust. The presence of both mafic and felsic magmas in the Princeton Group provides a unique opportunity to examine how adakitic magmas with greatly differing bulk compositions relate to one another, and to their geodynamic setting.

This paper presents results from a detailed examination of the Princeton Group, the most southwestern part of the Challis–Kamloops belt in Canada. Detailed field work and sampling were carried out near two well-exposed sections of Princeton Group at Agate Mountain and near Flat Top Mountain, both of which are southeast of Princeton, BC. These areas are composed of lavas, high-level intrusions, and pyroclastic rocks and are interpreted to be the eroded and uplifted remnants of larger volcanoes. Field, petrographic, geochronologic and geochemical data from these and other areas are provided, and are integrated with previous work. Together, they lead to a new tectono-magmatic model for Eocene magmatism in western North America and provide a new interpretation for the origin of their adakitic signature.

2. Geological setting

The North American Cordilleran orogen is largely a product of accretion of pericratonic and allochthonous terranes, mainly of late-Paleozoic to Mesozoic age, to the western margin of Laurentia (Monger and Price, 2002; Dickinson, 2004). The Princeton Group is located in the Intermontane belt, which is comprised of supracrustal and intrusive rocks that were affected by Mesozoic contractional and Tertiary transtensional deformation (Monger, 1985). The exposed basement to the Princeton Group is composed largely of Mesozoic arc rocks and subordinate Paleozoic rocks that have an oceanic affinity and are isotopically juvenile (Monger, 1989; Monger and McMillan, 1989; Ghosh, 1995). Contrary to the isotopic evidence, geophysical imaging indicates that rocks with affinity to ancestral North America may continue beneath the Princeton Group in the lower crust as a westward tapering wedge (Clowes et al., 1995).

The Princeton Group is an assemblage of volcanic and clastic sedimentary rocks exposed in a belt of discontinuous outliers that extends from the United States–Canada border north to Merritt BC, over a width of approximately 45 km and a length of about 150 km (Fig. 2; Monger, 1989; Monger and McMillan, 1989). The volcanic rocks include tuff, breccia and lava that range in composition from basaltic andesite to rhyolite. Aphyric andesitic to dacitic sills have locally inflated stratigraphic sections by up to two times their original thickness. Epiclastic sedimentary rocks are dominated by conglomerate, sandstone, siltstone and coal (Williams and Ross, 1979; McMechan, 1983; Read, 2000).

Eocene magmatic activity and sedimentation in the Challis–Kamloops belt occurred during an interval of widespread normal and dextral strike–slip faulting in British Columbia, Washington, and Idaho (Fig. 2; Ewing, 1980; Monger, 1985; Parrish et al., 1988). Block faulting influenced the deposition and preservation of the volcanic and sedimentary rocks of the Princeton Group, with the majority of workers concluding that the sedimentary outliers were deposited as discrete, unconnected basins with little lateral continuity. For example, thick

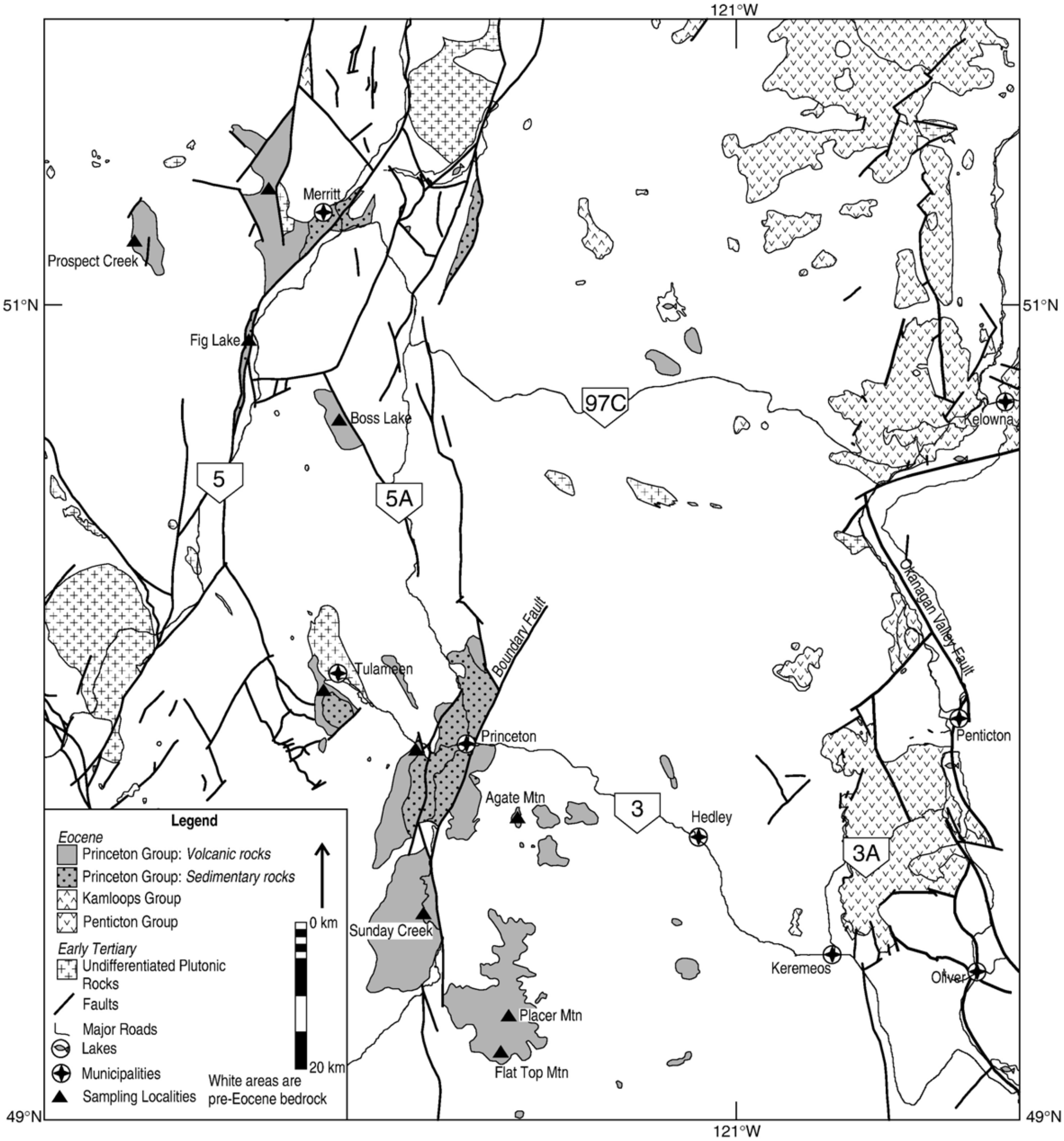

Fig. 2. Map of the Princeton Group and related Eocene units and features. The approximate positions of important sampling locations (as discussed in text) are indicated by a triangle, but for accurate positions refer to co-ordinates given in Appendix A. Features are adapted from Massey et al. (2005), Monger (1989), and Monger and McMillan (1989).

accumulations of sedimentary and volcanic rock in the fault-bounded Fig Lake graben (Thorkelson, 1989) and the Princeton Basin (McMechan, 1983) each cannot be correlated with deposits elsewhere in the Princeton Group and likely represent local, fault-bounded features with little lateral continuity. Thus, the current distribution of Princeton Group sedimentary outliers probably reflects the locations of original, variably restricted depositional centres, many of which were fault controlled. Primarily volcanic outliers like the ones examined in detail for this study, however, represent the erosional remnants of constructional volcanic centres and are not obviously fault controlled.

The Princeton Group lies south and west of the coeval Kamloops Group (Ewing, 1981a,b; Breitsprecher, 2002) and Penticton Group (Fig. 2; Church, 1973), respectively. The Kamloops Group is a volcanic arc-like assemblage of mafic, intermediate, and felsic volcanic rocks with subordinate intercalated non-marine sedimentary rocks (Ewing, 1981b). The Penticton Group is similar to the Kamloops Group, but also contains additional alkaline, intraplate-like lavas near its base (Dostal et al., 2003) and correlates with parts of the Klondike Mountain and the Sanpoil Volcanic formations of the Colville Igneous Complex in Washington (Church, 1973; Morris et al., 2000; Dostal et al., 2003; McClaughry and Gaylord, 2005). The separation of Eocene-age packages of volcanic rocks in southern BC from each other (i.e., Princeton–Kamloops–Penticton) is largely the result of a geographically-based historical usage of nomenclature rather than based on lithologic character or superposition of one succession over another (Breitsprecher, 2002). In this study we do not attempt to redefine the stratigraphic nomenclature and follow the traditional geographic distinctions of Monger (1989) and Monger and McMillan (1989).

The stratigraphy of the Princeton Group (Rice, 1947) was defined on the basis of detailed mapping near the town of Princeton (e.g. Camsell, 1913; Rice, 1947; Shaw, 1952; McMechan, 1983; Read, 2000) and divided into two formations: a lower, primarily volcanic unit named the Cedar Formation (Camsell, 1913) and an upper, sedimentary and volcanic succession named the Allenby Formation (Shaw, 1952). Although the formations are well-defined near the town of Princeton, distinguishing them away from the type area is problematic due to an unclear lithologic distinction between volcanic facies of each formation and the lack of demonstration of lateral continuity (Read, 2000). Therefore, in this study the volcanic rocks of the Cedar Formation are not differentiated from those in the Allenby Formation.

3. Princeton Group volcanism

3.1. Agate Mountain

A 135 m-thick section is exposed in the west-facing cliff-face of Agate Mountain, approximately 12 km southeast of Princeton (Fig. 3). The section consists of flat-lying lava flows, tephra and sills with basaltic andesite to andesite compositions. About half of the section is tephra, most of which is a coarse, moderately well sorted and poorly stratified, red-weathering pyroclastic breccia composed of scoriaceous to dense bombs and lesser lapilli. Subordinate, finer-grained tephra occurs in three horizons of metre-scale, well sorted, red-weathering, planar bedded layers of lapillistone and tuff. Lava flows occupy 13% of the section and are concentrated near the bottom. They are generally dark grey weathering, 5–7 m thick, and have thin, rubbly flow-tops. The sills are more silicic than the flows, occupy 20–40% of the section and range up to 30 m thick. They

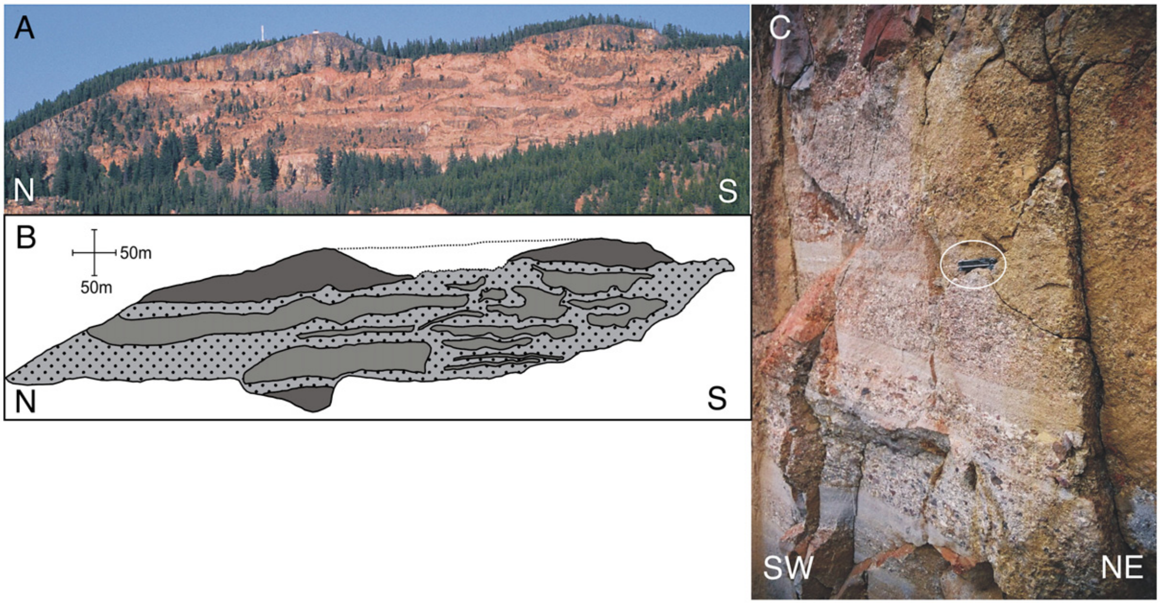

Fig. 3. Representative geological features of the Princeton Group, see Fig. 2 for location. A, B) Photograph and interpretive sketch of prominent west-facing cliff at Agate Mountain, dark grey units are andesitic sills, light grey units are mafic flows and stippled areas are tephra. C) Interbedded lapillistone and tuff near Flat Top Mountain. Folding knife (circled) for scale.

are mostly concordant with the stratigraphic layering and range from tabular to lensoidal, but some have irregular shapes and are locally discordant. Both the lavas and the sills are sparsely porphyritic. The lavas have a phenocryst assemblage of olivine + pyroxene + magnetite, with olivine predominant, and a nearly holocrystalline groundmass of plagioclase + clinopyroxene + magnetite. The sills have an assemblage of pyroxene + plagioclase + olivine with a hypocrystalline groundmass of plagioclase + clinopyroxene + magnetite.

We interpret the Agate Mountain exposure as a section through the lower part of a stratovolcano that was subsequently inflated by the injection of sills. The scoria-rich breccias are interpreted to be the slightly reworked deposits of eruptions from a nearby vent, and the well-bedded tuffs and lapillistones are interpreted to be fallout deposits from sustained eruptive columns (e.g. Riedel et al., 2003; Valentine et al., 2005). Based on their chemical and petrographic characteristics, we interpret the lavas to be effusions of separate batches from the same parental magma that periodically poured down flanks of the cone. The sills represent chemically more evolved, more viscous magmas that were injected into the section, probably after the volcano had grown and the Agate Mountain section was buried beneath a greater thickness of volcanic strata.

3.2. Flat Top Mountain

Approximately 200 m of tephra and trachyandesite are exposed on a southeast facing cliff two km east of Flat Top Mountain in one of the southernmost exposures of the Princeton Group (Fig. 3). Tephra, including very coarse pyroclastic breccia, tuff and lapilli-tuff, makes up the basal 75 m of the section. Clasts in pyroclastic breccia are poorly sorted and composed of altered aphyric to sparsely porphyritic andesite (similar to exposed coherent volcanic rock) and range in size from >1 m to 10 cm. Tuff and lapilli-tuff are well-bedded, well sorted and composed of ash or angular fragments of andesite, similar to that of the pyroclastic breccia.

Overlying the tephra is a 125 m-thick, concordant body of clinopyroxene trachyandesite that extends over an area of at least 1 km^2. The trachyandesite has crude vertical columnar joints and displays a crude horizontal layering defined by sets of columnar joints separated by horizontal bands of more fractured rock or by subtle changes in weathering colour and resistance to weathering. The unit is interpreted as either a sill or thick flow that may have been inflated by sill-like injections of magma prior to complete crystallization.

Other exposures in the vicinity of the Flat Top section include (a) thick (>75 m) units of columnar-jointed, highly porphyritic hornblende–plagioclase dacite containing hornblende–gabbro xenoliths and (b) smaller bodies of weakly porphyritic plagioclase–hornblende dacite. Both unit types appear to extend over 3 km and are interpreted as volcanic domes or cryptodomes.

The volcanic rocks at and near Flat Top Mountain are most likely the remnants of a composite volcano. The coarse pyroclastic breccia is interpreted as the product of collapse and minor reworking of the andesite-dominated volcanic flanks. The well-bedded lapilli-tuff and tuff are interpreted as fall-out deposits resulting from eruptions at a nearby vent. Proximity to basement rocks and the presence of high-level intrusive rocks suggest that uplift has exposed the roots of the volcanic centre, and that later faulting has disrupted continuity between outcrops and the relationship to basement rocks. Similar exposures of massive or heavily fractured to columnar-jointed andesite occur to the north around Placer Mountain, suggesting that the volcano or volcanic field extended at least 10 km northward.

4. Geochronology

4.1. Results

Three samples of hornblende, one whole rock sample and one groundmass sample were dated by the ^{40}Ar/^{39}Ar laser fusion technique at the Pacific Centre for Isotopic and Geochemical Research, Department of Earth and Ocean Sciences at the University of British Columbia, Canada (Table 1). The three hornblende separates yielded dates of 51.5 ± 2.1 Ma, 49.3 ± 1.4 Ma, and 50.3 ± 0.9 Ma, the groundmass separate yielded a date of 51.7 ± 1.6 Ma, and the whole rock yielded a date of 50.2 ± 0.4 Ma (all errors are at 2σ). Representative age spectra and an inverse isochron are presented in Fig. 4. Analytical methods and sample descriptions are presented in Appendix A.

4.2. Discussion

The new ^{40}Ar/^{39}Ar geochronological results presented here, in conjunction with other recent ^{40}Ar/^{39}Ar and U–Pb results (Villeneuve and Mathewes, 2005; Archibald and Mortensen,

Table 1
^{40}Ar/^{39}Ar data for volcanic rocks from the Princeton Group

Sample ID	Location	Rock type	Type	Plateau			Inverse isochron			Total fusion
				Date (Ma)	MSWD	^{39}Ar in plateau	Date (Ma)	MSWD	^{40}Ar/^{36}Ar$_i$	Date (Ma)
RBI-04-16-14-1B	Agate Mtn.	b.-andesite	Gm	54.6 ± 0.8	2.2	64%	[a]51.7 ± 1.6	1.4	428 ± 36	57.5 ± 1.0
RBI-04-24-6-1B	Friday Creek	dacite	Hbl	[a]51.5 ± 1.2	0.8	94%	52.6 ± 2.9	0.8	285 ± 28	49.7 ± 1.7
RBI-04-34-2-1	Lower Nicola	andesite	Hbl	[a]49.3 ± 1.4	0.4	100%	49.6 ± 1.6	0.4	291 ± 12	48.1 ± 2.3
RBI-04-35-3-1	Fig Lake	dacite	Hbl	[a]50.3 ± 0.9	0.7	100%	50.2 ± 1.0	0.8	297 ± 8	50.0 ± 1.6
RBI-04-36-1-1	Boss Lake	rhyolite	WR	[a]50.2 ± 0.4	1.0	90%	49.7 ± 1.2	1.0	307 ± 26	50.2 ± 0.4

All uncertainties at 2σ. Flux monitor is Fish Canyon Tuff sanidine with an age of 28.03 Ma (Renne et al., 1998).
Abbreviations: b.-andesite = basaltic andesite; Gm = groundmass; Hbl = hornblende; WR = whole rock.
[a] Interpreted as best estimate of crystallization age.

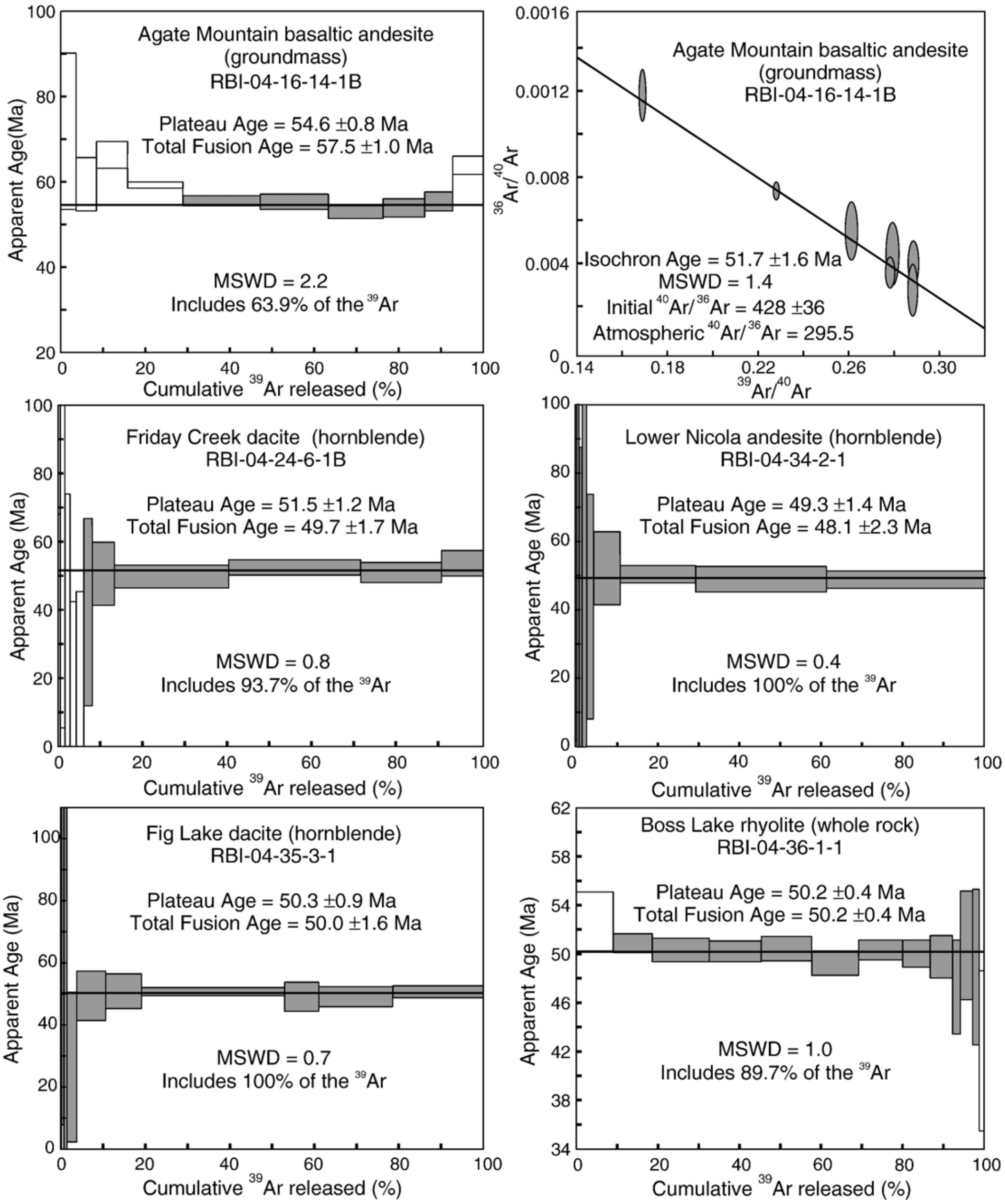

Fig. 4. ^{40}Ar/^{39}Ar degassing spectra of five Princeton Group samples. The data was processed and plotted using Isoplot 3.09 (Ludwig, 2003). The date determined from the plateau is the interpreted date of eruption for all samples except for RBI-04-16-14-1B, for which the date determined by the inverse isochron method is the interpreted eruptive age. The shaded release steps in the degassing spectra are the ones used in the plateau calculation. All uncertainties are reported at 2σ.

unpublished; Friedman and Thorkelson, unpublished), constrain the duration of volcanic activity in the Princeton Group to 53–47 Ma. This 6 m.y. duration of volcanic activity is similar to, but smaller than the range provided by previous work. There is no correlation between age and location or bulk composition. Available geochronological data for the Kamloops Group (compiled in Breitsprecher, 2002), Penticton Group and Colville Igneous Complex (Church, 1979; Church and Suesser, 1983; Mathews, 1989; Hunt and Roddick, 1990; Bardoux, 1993; Dostal et al., 2003; Church, unpublished) show that the duration of volcanic activity is 53–46 Ma and 54–47 Ma, respectively. Collectively, these data suggest that Eocene volcanism in southern BC was active during an interval lasting approximately 7 m.y. Most of the data for the Kamloops and Penticton Group are low precision K–Ar dates and do not permit analysis of temporal or compositional diachroneity.

The timing and duration of magmatism to the north, in central British Columbia is identical to that in the Princeton Group (Fig. 5). Grainger et al. (2001) studied the geochronology and local stratigraphic correlations of the Ootsa Lake Group in north-central BC and determined a duration of volcanic activity of 53–47 Ma. Additionally, these workers summarized previous work in the region and suggested that the age of most other volcanic units in north-central British Colombia (e.g. the

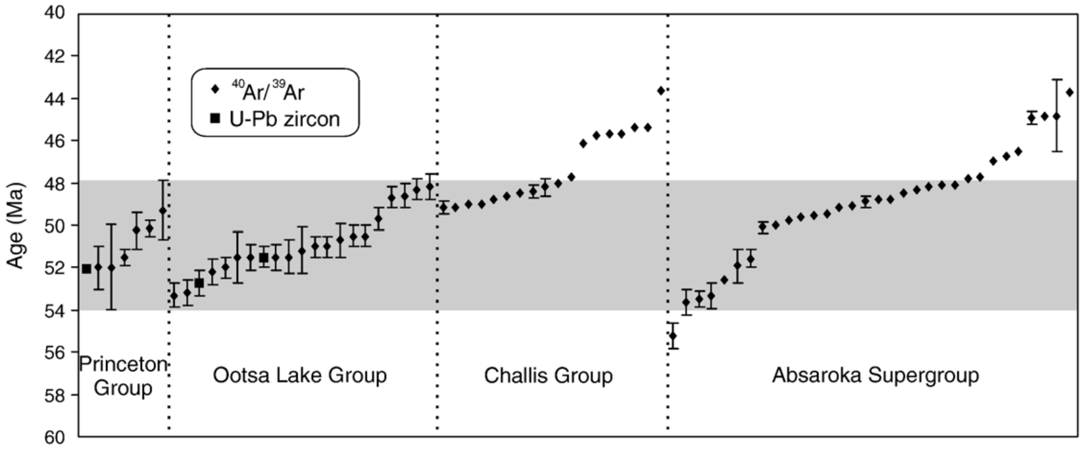

Fig. 5. Available $^{40}Ar/^{39}Ar$ and U–Pb zircon geochronology for the Princeton Group (K–Ar dates excluded), and volcanic fields of the Challis–Kamloops belt to the north (Ootsa Lake Group) and to the south (Challis Group and Absaroka Supergroup). Dates are compiled Janecke and Snee (1993); Janecke et al. (1997); Hiza (1999); Grainger et al. (2001); Feeley et al. (2002); and Feeley and Cosca (2003). Error bars represent uncertainties at 2σ, where error bars are not present the uncertainties are smaller than the symbol. Dates in this plot are as reported by the original authors and have not recalculated to a common monitor age.

Endako Group, Buck Creek Formation, and Newman Volcanics) falls into the same age bracket. Sparse geochronological results from small volcanic fields near the BC–Yukon border (Bennett Lake and Mount Skukum Volcanic Complexes; Morris and Creaser, 2003) suggest a slightly older history of 56–53 Ma, however more work needs to be done to confirm these ages.

South of the Princeton Group, the Challis Volcanic Field and Absaroka Supergroup (Fig. 1) have a very similar duration of magmatism. Janecke and Snee (1993) and Janecke et al. (1997) provided $^{40}Ar/^{39}Ar$ results from the Challis Volcanic Field showing that intermediate composition volcanic activity took place from 49–48 Ma and was followed by a pulse of explosive rhyolitic (possibly bimodal) volcanic activity from 46–45 Ma. The early phase of volcanism is coeval with magmatism in the Princeton Group, but the later phase is not and is probably related more to the mid-Eocene “ignimbrite flare up” (Humphreys, 1995) than the Challis–Kamloops event. Magmatism in the Absaroka Supergroup is apparently the most protracted in the Challis–Kamloops belt, lasting approximately 10 m.y. from 55–45 Ma (Hiza, 1999; Feeley et al., 2002; Feeley and Cosca, 2003), which overlaps both with magmatic activity to the north in the Princeton Group and central BC, as well as the late phase of volcanic activity in the Challis Volcanic Field.

5. Petrography

Mineral assemblages generally correlate with bulk composition. Rocks with less than 60 wt.% SiO_2 generally have a phenocryst assemblage of clinopyroxene ± olivine ± orthopyroxene ± magnetite, lack plagioclase phenocrysts, and have a groundmass assemblage of plagioclase + clinopyroxene + magnetite and minor devitrified glass. Rocks with SiO_2 contents from 60–70 wt.% are typically either strongly porphyritic (with as much as 50 vol.% phenocrysts) and have a phenocryst assemblage of plagioclase + hornblende + magnetite, or are only weakly porphyritic and have a phenocryst assemblage of plagioclase + clinopyroxene + magnetite (Fig. 6). Some dacites contain very small quantities of quartz and/or biotite phenocrysts. Trace amounts of clinopyroxene and hornblende are common in both hornblende-dominant and clinopyroxene-dominant rocks, respectively. In these more silicic samples, apatite and zircon are common trace minerals and the groundmass is composed of varying amounts of devitrified glass with microlites of plagioclase ± clinopyroxene ± magnetite. The only rhyolite sampled in this study (72 wt.% SiO_2) is weakly porphyritic and has small phenocrysts of K-feldspar, plagioclase, quartz, and biotite with a groundmass of devitrified glass and plagioclase microlites.

The phenocrysts have a wide range in textures. Olivine and pyroxene are typically subhedral and range from isolated grains to glomerocrysts. In one unit the orthopyroxene phenocrysts are strongly embayed. Where present, plagioclase is commonly oscillatory zoned, and sieve-textured, and locally has visible cores or intra-grain evidence for a resorption event in its history. Multiple plagioclase populations are common, as defined on the basis of texture, within a single sample. Hornblende is typically euhedral and optically unzoned. In some cases, individual crystals were in a clear reaction relationship with the melt, such as quartz xenocrysts reacting with melt to form clinopyroxene and orthopyroxene reacting with the groundmass to form hornblende.

Xenoliths of coarse-grained crystalline rock are locally abundant, particularly in some of the strongly porphyritic dacites. Most are less than 1 cm in diameter but range up to 3 cm. A small proportion of these xenoliths appear to be accidental crustal fragments and include foliated granitoid rocks. The majority of the xenoliths, however, have a massive, plutonic igneous texture and a mineral assemblage of plagioclase + hornblende + magnetite, identical to the host dacite or andesite. The hornblende is typically euhedral and the magnetite is commonly embayed. Both are enclosed by large, commonly oikocrystic, plagioclase that is unzoned except for narrow rims at their margins. In places, the groundmass projects into crystal-face bounded cavities within individual xenoliths, representing original magmatic porosity. Smaller xenoliths (<0.75 cm) with an identical mineral assemblage typically

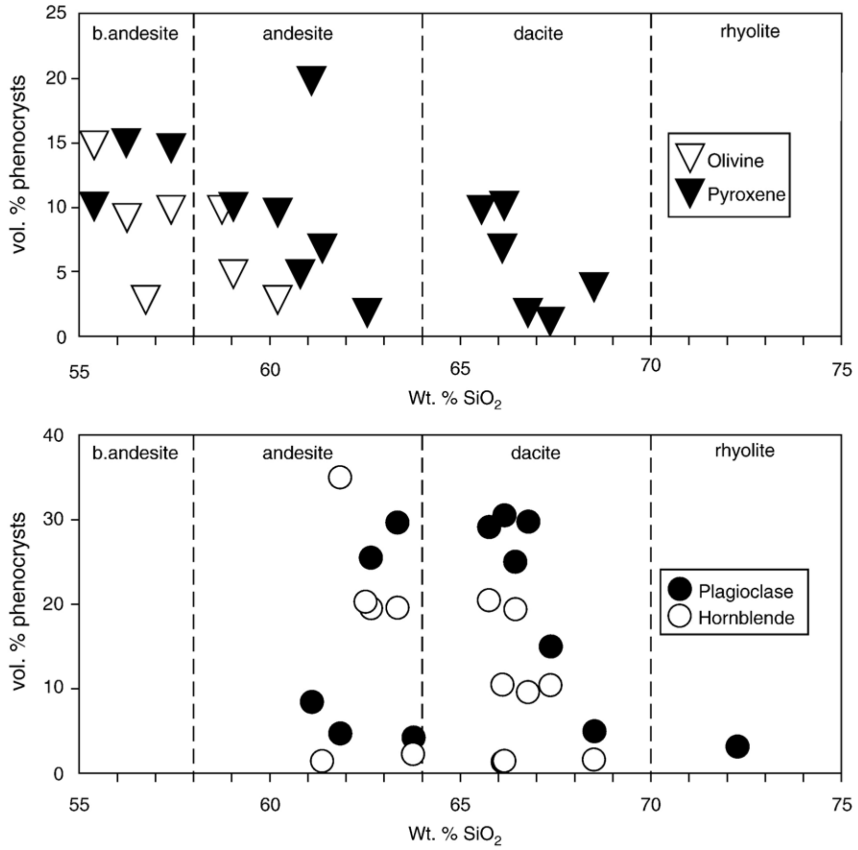

Fig. 6. Modal phenocryst abundances for volcanic rocks in the Princeton Group, expressed as volume percent of the total rock. All abundances are estimated visually. Orthopyroxene (opx) and clinopyroxene (cpx) are represented together, although generally cpx ≫ opx.

have different textures, which include those with equal-sized hornblende and plagioclase, and those comprised entirely of hornblende. These xenoliths are probably cognate with respect to the host rock.

6. Geochemistry and neodymium isotopes

6.1. Analytical techniques and uncertainties

Twenty-six rock samples were selected for chemical analysis and a subset of seven was selected for Nd isotopic analysis. Samples that were free of secondary minerals and amygdules were selected and chipped clean of weathered surfaces in the field. Seven of the chemical samples were from Agate Mountain, eleven samples were from the region near Flat Top Mountain and Placer Mountain, two were from the Sunday Creek region (which complement the four previously published by Breitsprecher, 2002), and the remaining six samples were from other localities to the north and northwest. The samples for Nd isotopic analysis were selected to represent a broad geographic and compositional range.

Major element and trace element concentrations were analyzed at commercial laboratories (ACTLABS [$n=25$] and ALS Chemex [$n=1$]) and are reported in Table 2, where all major element oxides are normalized to 100% on an anhydrous basis. Major elements (SiO_2, Al_2O_3, MgO, K_2O, Fe_2O_3, Na_2O, P_2O_4, TiO_2, MnO, and P_2O_5) and selected trace elements (Ba, Sr, Y, and V) were determined by fusion ICP-OES (inductively coupled plasma optical emission spectroscopy), Sc was determined by INAA (instrumental neutron activation analysis) and all other trace elements, including the lanthanides, were determined by ICP-MS (inductively coupled plasma mass-spectrometry). Samples were analyzed along with reference materials SY-2 syenite, MRG-1 gabbro, W-2 diabase, and WMG-1 gabbro. Uncertainties were calculated based on the reproducibility of eight pairs of duplicate samples (Ickert, 2006), nearly all uncertainties are <10% and most are <3% (Table 2). Relative uncertainties for Ta, Cs, Lu, Pb, and Mo are >10%. Concentrations of elements and oxides (including K_2O, Ba and Sr) do not correlate with loss-on-ignition (LOI), suggesting that low-temperature alteration has not significantly affected the chemistry of these samples.

Neodymium isotopic compositions were determined at the Pacific Centre for Isotopic and Geochemical Research, Department of Earth and Ocean Sciences, University of British Columbia, and are reported in Table 3. The analyses were carried out by thermal ionization mass-spectrometry (TIMS) on a Finnigan Triton mass spectrometer, following the methodology of Weis et al. (2005). The average $^{143}Nd/^{144}Nd$ of the La Jolla standard run during the analytical session was 0.511853±6 ($n=11$).

Table 2

Sample	RBI-04	RBI-04	RBI-04	RBI-04	RBI-04	RBI-04	RBI-04	RBI-04	RBI-04	RBI-04	DM-04	RBI-05	RBI-04	RBI-04	RBI-04	RBI-04	RBI-04	RBI-04	RBI-04	RBI-04	RBI-04	RBI-04	RBI-04	RBI-04	RBI-04	RBI-04	
	37-8-2	19-3-1	20-3-2	21-2-1	21-3-1	22-1-1	30-2-1	31-1-1	31-1-2	32-2-1	18-1-1	02-2-1	15-10-1	15-12-1	15-13-1	16-14-1	16-17-1	12-1-1	17-3-1	36-1-1	23-3-1	24-6-1	25-1-1	34-2-1	39-1-1	37-5-1	
Locality	PC	FT/P	FT/P	FT/P	FT/P	FT/P	FT/P	FT/P	FT/P	FT/P	FT/P	FT/P	AgM	AgM	AgM	AgM	AgM	AgM	AgM	BL	SC	SC	Tul	Mer	Pr	PC	
Rock type	b.and	and	dac	dac	and	dac	t.and	dac	dac	dac	dac	t.and	t. and	and	and	b. and	and	t. and	b.t. and	rhy	dac	dac	and	and	dac	and	2σ error
SiO_2 (wt.%)	56.23	62.55	66.15	63.75	61.85	66.77	61.37	68.50	66.42	67.35	65.76	57.84	61.09	59.04	58.74	56.74	60.80	57.41	55.39	72.27	66.10	63.35	60.20	62.65	65.55	61.08	0.4
Al_2O_3 (wt.%)	15.25	16.85	15.54	16.99	15.69	15.51	15.01	15.72	15.75	15.78	15.82	16.60	15.78	16.24	16.68	15.61	15.87	14.95	14.68	14.73	17.36	16.28	15.69	16.68	15.55	15.69	0.1
FeO^T (wt.%)	6.08	4.64	3.96	4.55	4.94	3.65	4.84	2.88	3.81	3.31	3.94	5.83	5.02	5.55	6.58	6.46	5.47	6.16	7.05	2.00	3.60	5.04	5.65	4.87	4.25	5.15	0.04
MnO (wt.%)	0.11	0.08	0.05	0.08	0.09	0.07	0.08	0.02	0.04	0.04	0.07	0.06	0.07	0.23	0.13	0.11	0.06	0.10	0.11	0.03	0.04	0.06	0.10	0.05	0.05	0.09	0
MgO (wt.%)	9.50	3.00	2.22	2.07	3.74	2.27	4.27	1.49	2.70	1.88	2.27	5.03	4.09	3.60	4.00	6.70	4.00	6.22	7.62	0.62	0.84	3.08	4.43	3.22	2.29	5.22	0.04
CaO (wt.%)	7.54	5.28	4.32	5.17	6.45	4.06	6.07	3.47	4.19	3.83	5.03	6.56	6.14	8.56	7.13	7.98	6.41	7.62	7.94	2.31	4.22	5.23	7.36	5.28	4.23	6.01	0.06
Na_2O (wt.%)	3.14	4.52	4.45	4.54	4.05	4.52	4.51	4.65	4.38	4.58	4.38	4.67	4.43	4.15	4.05	3.86	4.18	4.13	4.00	4.09	4.85	4.18	4.39	4.20	4.58	3.84	0.04
K_2O (wt.%)	1.24	2.16	2.46	2.04	2.23	2.41	2.68	2.65	2.00	2.52	1.96	1.95	2.31	1.55	1.48	1.44	2.17	2.08	1.61	3.53	2.23	1.79	1.05	2.23	2.44	2.12	0.02
TiO_2 (wt.%)	0.75	0.66	0.62	0.53	0.70	0.56	0.63	0.47	0.54	0.53	0.56	0.89	0.73	0.81	0.88	0.82	0.75	0.81	1.15	0.31	0.47	0.71	0.77	0.63	0.77	0.60	0.01
P_2O_5 (wt.%)	0.16	0.25	0.24	0.27	0.26	0.17	0.54	0.15	0.18	0.18	0.21	0.58	0.34	0.27	0.32	0.27	0.29	0.53	0.45	0.11	0.29	0.27	0.35	0.20	0.28	0.19	0.06
LOI (wt.%)	1.89	1.98	1.83	1.11	3.41	1.35	1.43	1.47	2.20	1.29	2.55	1.82	0.96	3.26	3.69	1.92	2.10	1.40	2.23	0.70	2.62	2.88	2.55	2.97	2.13	1.45	–
Total (wt.%)	98.65	98.79	99.90	99.02	99.74	99.43	99.14	100.33	99.68	99.58	99.03	99.86	99.23	99.63	98.78	99.59	99.09	98.54	98.88	99.84	99.14	98.86	99.27	99.07	98.65	99.47	–
Mg#	78	59	56	51	63	58	67	54	62	56	57	66	65	59	58	70	62	70	71	41	35	58	64	60	55	70	
Cu (ppm)	71	36	61	15	45	56	11	53	31	48	24	35	25	53	44	48	36	101	61	53	11	26	56	46	69	65	2
Ni (ppm)	239	31	28	19	60	33	53	15	25	19	20	66	93	141	167	181	117	171	179	5	2	12	92	52	58	112	2
Pb (ppm)	5	3	8	bd	10	4	18	6	bd	bd	16	28	24	8	4	7	20	12	11	15	9	10	7	8	12	5	4
Ba (ppm)	485	1123	1081	967	892	976	1974	1106	829	1025	849	1585	1468	960	800	690	1242	1168	1033	1402	1045	746	900	877	1073	872	14
Rb (ppm)	22	39	48	38	39	47	48	56	36	52	32	38	30	25	23	22	29	26	20	102	39	29	34	48	42	44	0.7
Sr (ppm)	704	1053	675	910	794	629	1991	651	680	670	754	2020	1731	969	1022	985	1455	1742	1419	411	980	588	1312	867	787	802	9
Zr (ppm)	85	120	125	118	102	116	122	137	96	142	86	123	125	101	97	93	117	125	144	141	128	98	106	84	144	100	4
Y (ppm)	12	10	9	11	10	8	14	8	8	8	10	17.2	11	11	12	11	10	12	15	6	10	14	11	9	8	10	0.8
V (ppm)	150	106	95	85	125	85	99	71	85	82	90	144	124	144	155	146	130	134	152	32	61	124	126	100	84	122	2
Co (ppm)	47.1	18.9	15.3	13.5	23.2	15.1	22.4	11.1	16.3	13.8	13.5	20.7	21.8	28.6	33.0	35.8	23.7	30.5	35.3	6.8	10.1	20.4	30.6	19.4	17.3	29.8	1
Cr (ppm)	663	38	93	38	157	107	106	45	78	56	88	160	146	376	419	405	226	302	423	26	7	35	250	91	105	255	4
Mo (ppm)	2	bd	7	10	14	7	30	5	8	12	bd	Bd	15	9	14	9	13	22	17	bd	16	10	10	bd	bd	bd	6
Sc (ppm)	29.9	13.0	11.7	9.2	15.3	10.2	11.9	7.8	11.1	8.8	12.1	Nd	13.1	19.4	20.5	20.5	15.8	18.1	21.9	4.7	4.6	15.2	15.5	14.5	11.2	19.4	0.4
Nb (ppm)	2.9	4.2	2.3	3.2	3.1	2.2	14.5	3.4	2.8	2.5	2.6	11	3.9	3.0	3.0	2.8	3.1	5.6	5.4	4.4	4.0	3.3	3.3	1.9	3.5	2.3	0.2
Cs (ppm)	0.8	1.1	0.8	1.0	0.5	0.8	0.9	0.9	0.8	0.9	0.9	0.5	0.5	0.9	0.8	0.2	0.6	0.6	bd	2.8	0.7	0.8	3.3	0.9	0.8	0.9	0.2
La (ppm)	12.1	23.9	22.0	19.6	20.1	17.4	93.2	24.3	14.2	22.0	12.7	69.3	26.2	17.3	18.4	17.7	22.8	36.5	41.0	21.8	25.9	15.4	23.6	14.9	24.5	16.5	0.6
Ce (ppm)	26.4	47.6	39.0	37.7	40.6	36.1	174	45.2	28.4	42.0	25.8	137	55.7	37.0	40.2	38.3	49.0	76.2	83.7	40.4	49.6	31.8	52.0	30.9	49.1	33.9	1.2
Pr (ppm)	3.40	5.73	5.22	4.68	5.04	4.24	19.2	5.04	3.55	4.84	3.27	16	7.35	4.88	5.22	5.00	6.42	9.83	10.2	4.36	5.83	3.92	6.56	3.93	5.80	4.24	0.1
Nd (ppm)	14.6	22.1	20.3	18.4	20.5	16.6	71.0	18.7	14.8	18.4	13.5	60.9	30.6	20.8	22.5	21.3	26.8	40.0	40.0	15.5	22.1	16.1	27.3	16.5	22.8	16.9	0.6
Sm (ppm)	3.32	4.24	4.11	3.61	4.21	3.37	11.3	3.32	3.07	3.52	2.99	9.8	6.49	4.39	4.77	4.53	5.62	7.52	7.60	2.86	3.96	3.60	5.33	3.44	4.30	3.43	0.2
Eu (ppm)	1.01	1.15	1.05	0.985	1.09	0.882	2.59	0.807	0.818	0.887	0.844	2.2	1.65	1.27	1.35	1.30	1.51	1.98	1.97	0.647	1.06	1.04	1.39	0.938	1.20	0.974	0.06
Gd (ppm)	2.70	3.09	2.95	2.88	3.13	2.43	5.98	2.18	2.32	2.35	2.28	7.3	4.44	3.37	3.47	3.45	4.09	4.87	5.42	1.81	2.75	3.08	3.65	2.56	2.95	2.57	0.1
Tb (ppm)	0.44	0.41	0.41	0.43	0.43	0.33	0.73	0.30	0.36	0.32	0.37	0.8	0.52	0.45	0.50	0.47	0.52	0.60	0.70	0.24	0.39	0.50	0.49	0.38	0.44	0.39	0.02
Dy (ppm)	2.36	2.02	1.89	2.11	2.10	1.64	2.90	1.40	1.70	1.47	1.71	3.4	2.34	2.23	2.24	2.28	2.23	2.54	3.03	1.07	1.88	2.57	2.19	1.82	1.83	1.83	0.08
Ho (ppm)	0.44	0.37	0.32	0.39	0.37	0.29	0.47	0.24	0.29	0.25	0.31	0.6	0.38	0.41	0.40	0.39	0.39	0.42	0.52	0.17	0.34	0.50	0.36	0.32	0.30	0.33	0.02
Er (ppm)	1.32	1.07	0.93	1.23	1.09	0.86	1.31	0.73	0.87	0.75	0.91	1.8	1.06	1.10	1.07	1.16	1.09	1.14	1.50	0.48	1.07	1.59	1.01	0.95	0.91	0.99	0.04
Tm (ppm)	0.192	0.153	0.135	0.193	0.168	0.123	0.181	0.105	0.127	0.109	0.130	0.2	0.151	0.168	0.159	0.165	0.157	0.159	0.211	0.067	0.152	0.237	0.142	0.144	0.127	0.143	0
Yb (ppm)	1.22	1.02	0.84	1.25	1.04	0.72	1.14	0.67	0.77	0.67	0.85	1.4	0.94	1.00	1.06	1.09	1.06	1.05	1.34	0.44	1.10	1.46	0.94	0.87	0.76	0.99	0.04
Lu (ppm)	0.18	0.16	0.13	0.21	0.16	0.11	0.16	0.11	0.11	0.10	0.12	0.20	0.15	0.15	0.15	0.15	0.15	0.15	0.19	0.06	0.15	0.21	0.13	0.13	0.10	0.14	0.06
Hf (ppm)	2.2	3.2	3.3	3.1	3.0	3.2	3.3	3.7	2.7	3.7	2.6	4	3.5	2.7	2.6	2.4	3.2	3.0	3.6	3.8	3.4	2.9	3.7	2.4	3.9	2.8	0.1
Ta (ppm)	0.19	0.28	0.16	0.21	0.20	0.16	0.53	0.21	0.18	0.16	0.18	Bd	0.19	0.17	0.17	0.16	0.19	0.21	0.26	0.45	0.25	0.19	0.18	0.13	0.21	0.13	0.04
Th (ppm)	1.82	4.08	5.36	3.98	3.93	4.94	9.07	6.56	3.05	5.96	2.37	7	4.30	2.20	2.35	2.27	4.11	3.63	3.56	8.01	4.46	2.74	2.74	3.10	4.97	3.31	0.08
U (ppm)	0.86	1.71	2.08	1.68	1.62	1.98	2.38	2.34	1.39	2.13	1.21	2	3.27	1.06	0.92	0.89	3.02	1.32	0.93	3.71	1.57	1.24	1.10	1.42	1.77	1.52	0.02

Abbreviations: AgM: Agate Mountain; BL = Boss Lake; SC = Sunday Creek; Tul = Tulameen; Mer = Merritt; Pr = Princeton; PC = Prospect Creek; FT/P = Flat Top Mountain and Placer Mountain; t.and = trachyandesite; and = andesite; b.and = basaltic andesite; b.t.and = basaltic trachyandesite; rhy = rhyolite; dac = dacite; nd = no data; bd = below detection.

Major elements (wt.% oxides) are normalized to 100% on an anhydrous basis. Original, pre-normalized totals are presented.

Table 3
Nd isotope date for volcanic rocks from the Princeton Group

Sample	Unit	$^{143}Nd/^{144}Nd_m$	$^{147}Sm/^{144}Nd$	$^{143}Nd/^{144}Nd_{50}$	εNd_{50}	T_{DM}
RBI-04-15-10-1	Agate Mountain	0.512896±7	0.1284	0.512854	5.5	453
RBI-04-16-14-1	Agate Mountain	0.512899±10	0.1277	0.512857	5.5	444
RBI-04-36-1-1	Boss Lake	0.512914±7	0.1131	0.512877	5.9	358
RBI-04-23-3-1	Friday Creek	0.512760±4	0.1094	0.512724	2.9	569
RBI-04-37-8-2	Prospect Creek	0.512945±6	0.1367	0.512900	6.4	405
RBI-04-31-1-1	Flat Top Mountain	0.512847±8	0.1067	0.512812	4.7	431
DM-04-18-1-1	Flat Top Mountain	0.512867±6	0.1344	0.512823	4.9	542

Uncertainties reported at 2σ. Concentrations and ratios of Sm and Nd are from Table 4. εNd_{50} is the part per 10,000 variation at 50 Ma from a chondritic reservoir with present day $^{147}Sm/^{144}Nd=0.1966$ and $^{143}Nd/^{144}Nd=0.512638$. T_{DM} is the model age, in Ma for extraction from a depleted mantle-type reservoir using the model of Goldstein et al. (1984).

6.2. Results

6.2.1. Major elements

Volcanic rocks from the Princeton Group exhibit a wide and continuous range in major element chemistry (Fig. 7). The SiO_2 contents range from 55–72 wt.% and MgO contents range from 0.62–9.50 wt.%. On a total-alkali vs. SiO_2 diagram (Fig. 7; Le Maitre, 2002) the rocks are classified as basaltic andesite, basaltic trachyandesite, andesite, trachyandesite, dacite and rhyolite. Andesite and dacite predominate. All samples are subalkaline (Irvine and Baragar, 1971), most are medium-K, and four samples are high-K (Fig. 7; Le Maitre, 2002). The whole suite exhibits relatively constant and low FeO/MgO, similar to that associated with calc–alkaline suites, although two samples from the Sunday Creek area (out of six from the suite) have significantly lower MgO contents than the others from the area and appear to be tholeiitic (Fig. 7; Miyashiro, 1974). They form a calc-alkalic to calcic suite (variation in the alkali–lime index is due to scatter in Na_2O and K_2O) according to the definition of Peacock (1931).

Some major oxides that partition strongly into or are essential constituents of mafic minerals (including MnO, MgO, and FeO) have strong negative correlations with SiO_2 content. In addition, TiO_2, which is incompatible in olivine and clinopyroxene (but moderately compatible in hornblende and very compatible in magnetite), also has a strong negative correlation with SiO_2. No obvious inflections in the patterns are present. Other major elements (e.g., K_2O, Na_2O, and Al_2O_3) correlate poorly with SiO_2, both within individual suites and within the Princeton Group as a whole.

The Mg# (molar $Mg/(Mg+Fe^{2+})\cdot 100$); FeO recalculated based on $Fe_2O_3/FeO=0.3$; Gill, 1981) of the Princeton Group volcanic rocks are unusually high for calc–alkaline volcanic suites. The Mg# varies from 92–27 with the vast majority greater than 50 (Fig. 8). Correspondingly, these rocks are in Fe–Mg equilibrium with olivine of a high forsterite content (calculated after Roeder and Emslie, 1970), ranging from Fo_{61} to Fo_{89} (excluding a very high-MgO sample that has accumulated orthopyroxene) although most are in Fe–Mg equilibrium with olivine of Fo_{80} to Fo_{89}. If calculations are performed assuming all Fe as Fe^{2+}, the equilibrium forsterite content in olivine decreases by 3–6 mol%.

6.2.2. Trace elements

Multi-element diagrams (normalized to normal mid-ocean ridge basalt: NMORB, Sun and McDonough, 1989) of volcanic rocks from the Princeton Group have broadly similar patterns to average upper continental crust and modern subduction-related volcanic rocks (Fig. 9). These features include positive anomalies in Pb and Sr, and negative anomalies in Nb, Ta, Hf, Zr, and Ti. These features are present at the entire compositional range.

The trace elements that are compatible in mafic phases (e.g., Ni, Cr, V, and Sc) have strong negative correlations with SiO_2 and generally have positive correlations with each other. For example, Ni concentrations range from relatively high values of ~175 ppm in olivine-bearing rocks from Agate Mountain, to <50 ppm in silicic andesites and dacites from elsewhere in the Princeton Group. Most trends have inflections at about 60 wt.% SiO_2, correlating with changes in phenocryst mineral assemblages from olivine and clinopyroxene dominated rocks to plagioclase and hornblende bearing rocks.

Many incompatible trace elements, including the high-field strength elements (HFSE; e.g., Zr, Hf, Nb, Ta), actinides (Th, U), and rare earth elements (La to Lu) correlate poorly with SiO_2. The large-ion lithophile elements Sr and Rb show weak negative and positive correlations respectively with SiO_2 and Ba have no correlation with SiO_2. The abundances of most HFSE are relatively low and constant at only about 1–2 times that of NMORB but concentrations of actinides, light rare earth elements (LREE: La, Ce, Pr and Nd), and LILE are highly elevated resulting in suprachondritic La/Nb, U/Nb, and Ba/Nb, common features in both average upper continental crust (Rudnick and Gao, 2003) and subduction-related magmas (Gill, 1981; Pearce and Peate, 1995). The concentrations of heavy rare earth elements (HREE: Er, Tm, Yb, and Lu) are particularly low and relatively constant at about 0.2–0.5 times NMORB, resulting in relatively high chondrite normalized ratios of light to heavy REE ($La/Yb_{cn}=6–56$).

6.2.3. Adakite and high-Mg# andesite

The Princeton Group contains abundant adakite and high-Mg# andesite. Adakites are defined as volcanic rocks (andesites and dacites sensu lato) with $SiO_2>56$ wt.%, $Al_2O_3>15$ wt.%, $Na_2O>3.5$ wt.%, Sr>400 ppm, Y<18 ppm, Sr/Y>40, Yb<1.9 ppm, and La/Yb>20 (Defant and Kepezhinskas, 2001). High-Mg# andesites (also referred to as high-Mg andesites) are defined as rocks with $SiO_2>54$ wt.% and Mg#>56 (Kelemen et al., 2003) and, although by definition they are not necessarily equivalent to adakites, are commonly

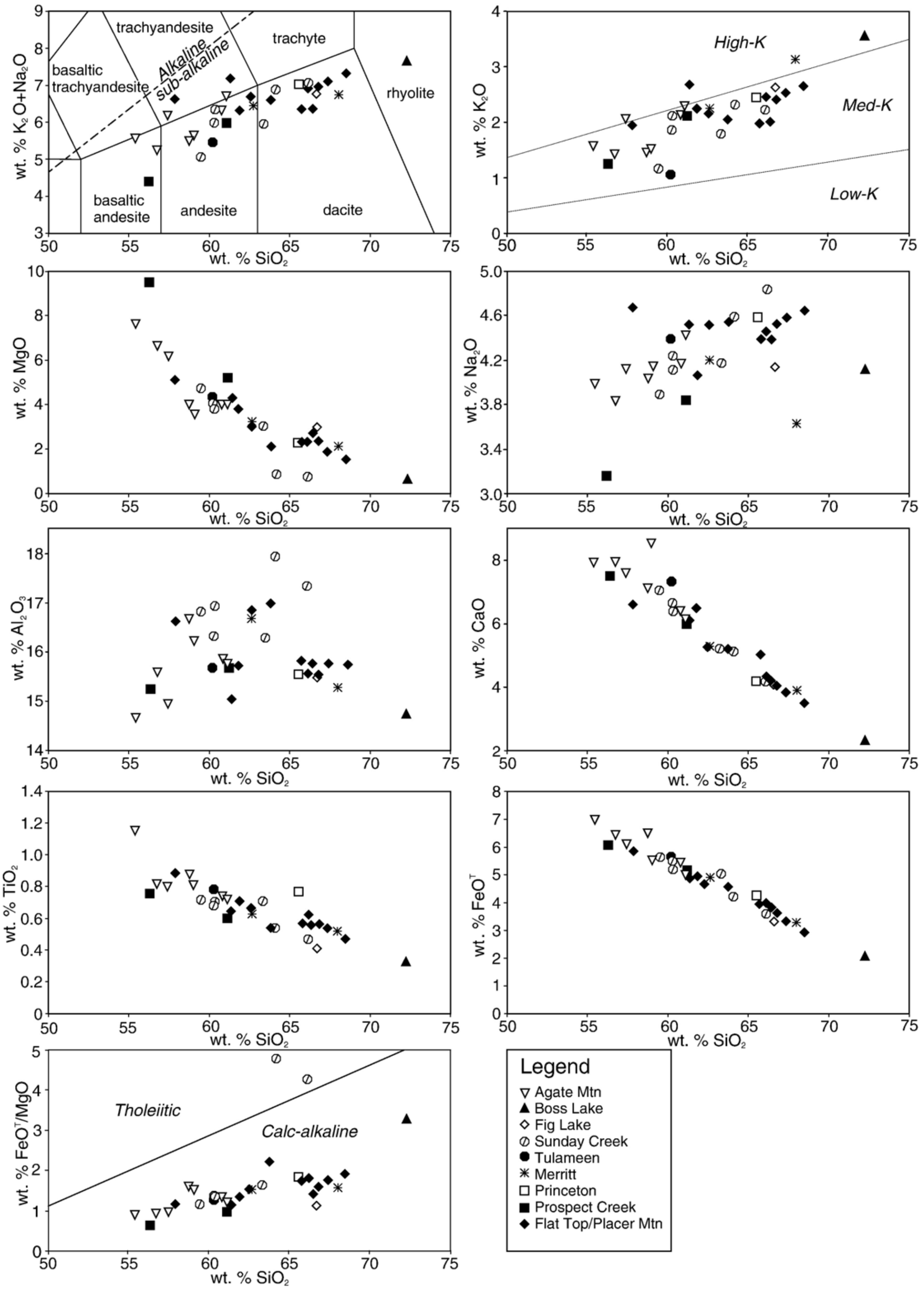

Fig. 7. SiO_2 variation (Harker) diagrams for major element oxides. Total alkali vs. silica (TAS) diagram in top left after Le Maitre (2002) and SiO_2 vs. FeO^T/MgO diagram after Miyashiro (1974). The 2σ uncertainties are typically smaller than the symbols.

adakitic or associated with adakites. Including those already identified by Breitsprecher et al. (2003), nearly half of all rocks analyzed in the Princeton Group are adakites and three-quarters are high-Mg# andesites. Three quarters of the adakites are also high-Mg# andesites.

Adakite and related high-Mg# andesite are intriguing classes of volcanic rock that are associated with controversial topics such as slab melting in subduction zones (Defant and Drummond, 1990), crustal differentiation (Atherton and Petford, 1993), crustal growth (Kelemen, 1995), and Archean plate tectonics (Martin,

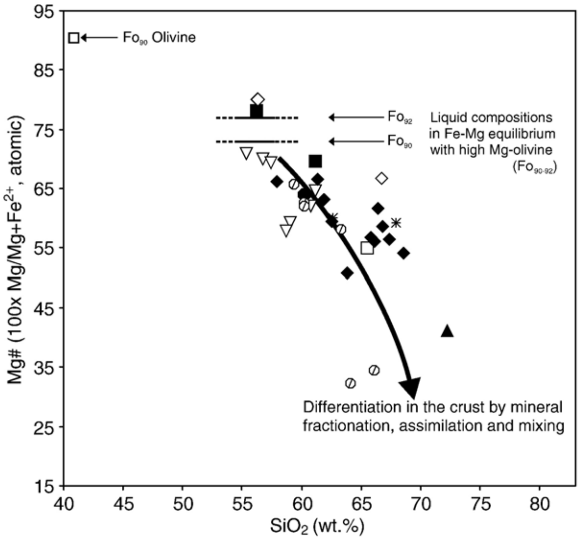

Fig. 8. Variation of Mg# with SiO_2. Liquid compositions in equilibrium with high-Fo olivine are calculated after Roeder and Emslie (1970). Whole rock compositions plotting above the equilibrium ratio for Fo_{92} olivine are probably affected by crystal accumulation. The arrow schematically represents the chemical evolution of the Princeton Group volcanic rocks as described in Section 6.3.

1999). Adakite in the Princeton Group was previously linked to slab-melting (Breitsprecher et al., 2003; Thorkelson and Breitsprecher, 2005) although that connection is challenged in this paper, and is discussed in detail, below.

6.2.4. Neodymium isotopes

Seven new Nd isotopic analyses of whole rocks were determined for the Princeton Group (Fig. 10; Table 3). Two previous Nd isotopic compositions were provided by Ghosh (1995) without accompanying major or trace element analyses. The range in εNd at 50 Ma (εNd_{50}) for the Princeton Group is from +1.2 to +6.4. Depleted mantle model ages representing the minimum time of extraction from the mantle (assuming a uniform composition mantle source) range from 350–750 Ma. Neodymium isotopes do not correlate with major element abundances, trace element ratios or indices of differentiation. For example, the lowest εNd_{50} values (+1.2 to +2.9) occur in Sunday Creek dacites with low Ni concentrations and Mg#, but the Boss Lake rhyolite has a relatively high εNd_{50} of +5.9, greater than a primitive olivine-bearing basaltic andesite at Agate Mountain (εNd_{50}=+5.5). Although the relatively high εNd_{50} values rule out a significant contribution from typical ancient continental crust or derivative sedimentary rocks, they do not rule out contributions from juvenile continental rocks with shorter crustal residence times such as rocks similar to the exposed Mesozoic basement. The range in εNd_{50} of the basement to the Princeton Group completely overlaps with that of the Princeton Group (Ghosh, 1995; Smith and Thorkelson, 2002; n=45). They are, however, significantly different than some alkaline rocks near the base of the nearby Penticton Group, the Yellow Lake Member, which has a range of εNd_{50} from −4 to −6 (Dostal et al., 2003).

6.3. Compositional variation in the Princeton Group: crystallization, assimilation, and source heterogeneities

The large compositional variations in the Princeton Group can be explained mainly by fractional crystallization, with subordinate assimilation of crustal material and magma mixing. Basaltic andesites and andesites, when compared to andesites and dacites, have higher concentrations of Ni, Sc and Cr, as well as higher MgO, FeO, and CaO. Mineral assemblages are dominated by olivine and clinopyroxene in these rocks (Fig. 6) and fractional crystallization of these minerals can account for the strongly negative trends on Harker diagrams. Furthermore, the co-variations between these elements change in concert with changes in the phenocryst assemblages. For example, as a function of SiO_2, Ni concentrations drop rapidly (from >170 ppm to <70 ppm) while olivine and clinopyroxene dominate the phenocryst assemblages. However, at about 60 wt.% SiO_2, when plagioclase and hornblende dominate the assemblages, the drop is less pronounced and the trend is more scattered. This change in trend can be attributed to the higher compatibility of Ni in olivine and clinopyroxene, compared to hornblende and plagioclase.

Quantitative modelling, by calculating Rayleigh fractional crystallization paths using the observed phenocryst assemblages, demonstrates that fractional crystallization is likely to have been the dominant process by which Princeton Group rocks are related (Fig. 11). The modelling calculates the changing abundances of Ni and SiO_2 by fractionation of observed phenocryst assemblages, where the fractionating assemblage varies with bulk composition (e.g., Fig. 6). The two curves in Fig. 11A show the results of fractional crystallization starting from two different primitive (olivine phyric, Mg#>60) Princeton Group magmas. Other compatible elements have inflections similar to those in Fig. 11A that also correlate with changes in phenocryst assemblages. Strontium concentrations, for example, vary widely in the plagioclase-free mafic rocks but steadily decrease once plagioclase becomes a major fractionating phase because Sr is compatible in plagioclase.

Variations in incompatible element abundances (e.g., some LILE, REE, HFSE, actinides) are also broadly consistent with fractional crystallization but the models are heavily dependant on the choice of parental magmas. Variations as a function of SiO_2 or compatible elements are generally scattered or show a weak increase (e.g., Th in Fig. 11B). These trends are understandable because incompatible element concentrations increase modestly as a result of low degrees of fractional crystallization (e.g., an increase by only a factor of ~1.4 at 30% crystallization). The strong dependency of incompatible element abundances in evolved magmas on the abundances in primitive magmas is illustrated quantitatively in Fig. 11B. Here, two fractional crystallization paths (calculated in the same way as those in Fig. 11A) have been calculated for Ni and Th from two different primitive lavas, each with a different Th content. In the calculated liquid-lines-of-descent, the large, primary, differences in Th contents are maintained over a large degree of fractional crystallization. Therefore, the scattered trends in incompatible element ratios against indices of differentiation, such as SiO_2 or Ni, can be understood as heterogeneity in the parental magmas,

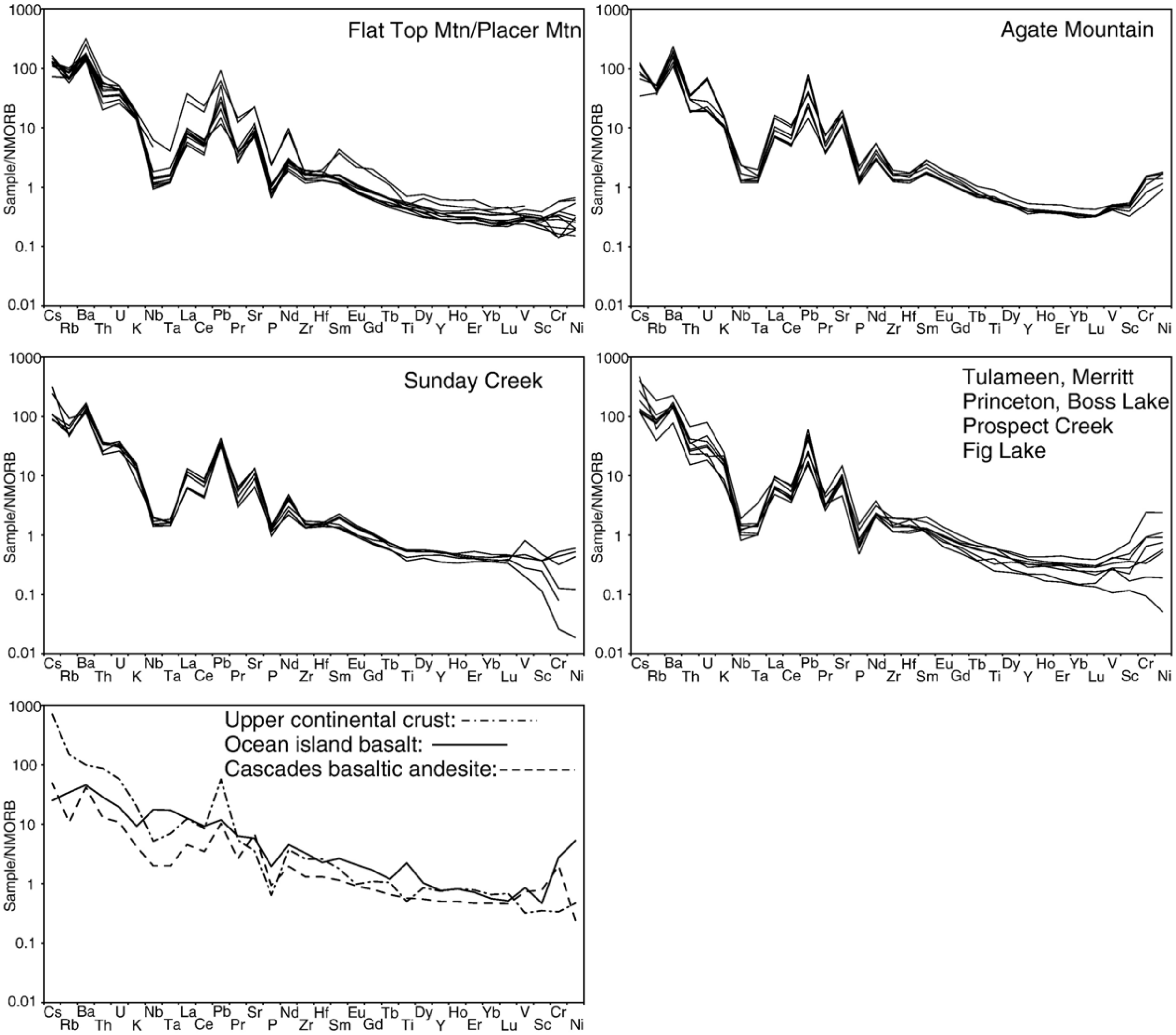

Fig. 9. NMORB (Normal Mid-Ocean Ridge Basalt; Sun and McDonough, 1989) normalized trace element diagrams. For reference, the upper continental crust composition of Rudnick and Gao (2003), a typical EM-1 ocean-island basalt from Pitcairn Island (sample 49DS-1 of Eisele et al., 2002; Hofmann, 2003), and a basaltic andesite from Mount Shasta (sample 82–94a of Grove et al., 2002; Ta calculated assuming a chondritic Nb/Ta of 17.6). See Fig. 2 for locations.

either as a function of source heterogeneity or as degree of melting in the source area.

Petrographic and isotopic evidence is also consistent with fractional crystallization as a dominant process in differentiation. The common presence of hornblende–gabbro xenoliths, interpreted as fragments of coeval plutonic rocks, is evidence that the magmas had partly crystallized prior to eruption. In addition, at Flat Top Mountain and Agate Mountain, where the Nd isotopic compositions of multiple samples are available, different units have identical isotopic compositions within error indicating that open-system processes such as assimilation and mixing do not dominate the differentiation mechanisms.

Petrographic evidence suggests that magma mixing and assimilation of crustal material may account for some of the compositional scatter in the Princeton Group volcanic rocks. For example, multiple textural populations of plagioclase are clear evidence for the mixing of different magmas. Similarly, the presence of accidental xenoliths and xenocrysts in reaction relationships with the host magma indicates assimilation of crustal rock. However, the typically non-linear chemical trends on some variation diagrams (such as Ni vs. SiO_2) indicate that magma mixing is likely to have played a minor role in magma differentiation, as mixing should produce linear trends on all variation diagrams. Assimilation with fractional crystallization (AFC; De Paolo, 1981) produces trends similar to fractional crystallization, especially at low ratios of mass assimilated to mass fractionated. AFC modelling predicts that the most chemically evolved rocks should have the most “crustal” or unradiogenic Nd isotopic signature. Although this characteristic is evident in highly differentiated dacite from Sunday Creek (Mg# = 32–35; $\varepsilon Nd_{50} = +2.7$ to $+2.9$) it is not true for the highly evolved rhyolite from Boss Lake (Mg# = 41; $\varepsilon Nd_{50} = +5.9$). The importance of assimilation relative to fractional crystallization, therefore, remains uncertain.

Heterogeneity of the highest Mg#, or most “primitive” magmas of the Princeton Group is an important factor in the variability of trace element abundances. Primitive magma heterogeneity is evident from mafic rocks (Mg# > 65) which

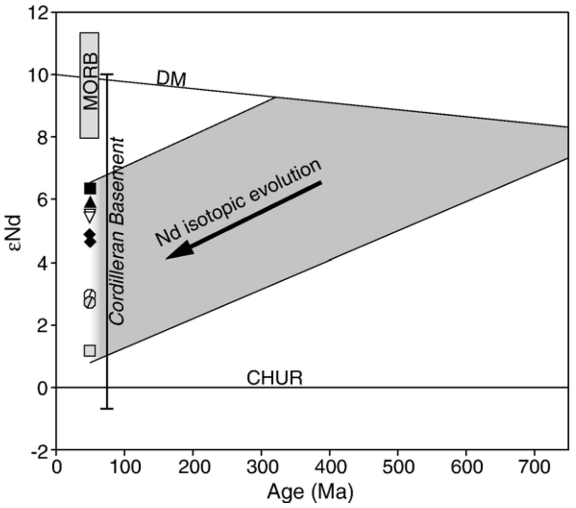

Fig. 10. εNd vs. time diagram. Symbols are as in Fig. 9, however grey symbols are data from Ghosh (1995). MORB field is the 2 standard deviation distribution for NMORB from the East Pacific Rise (http://www.petdb.org/). The Cordilleran Basement bracket is the 2 standard deviation distribution for basement rocks to the Princeton Group (Ghosh, 1995; Smith and Thorkelson, 2002). DM curve is from Goldstein et al. (1984). The field labelled Nd isotopic evolution is based on projecting the Nd isotopic compositions of Princeton Group rocks back in time assuming they had a present day Sm/Nd. CHUR stands for CHondritic Uniform Ratio.

display ranges in many trace element abundances that are nearly as high as those in the more evolved rocks. The variability in primitive rock compositions is therefore likely mantle-derived, rather than a consequence of crustal assimilation and fractionation. The adakitic character of the Princeton Group is, therefore, a primary feature rather than one generated by crustal-level processes such as assimilation, fractional crystallization or magma mixing. Constraints on the origins of primitive rocks in the Princeton Group are explored in more detail below.

7. Discussion

7.1. Adakite and high-Mg# andesite: petrogenetic and tectonic significance

Adakites were originally defined on the basis of rocks with compositions that were similar to theoretically predicted and experimentally derived compositions of melts of subducted oceanic crust (Kay, 1978; Defant and Drummond, 1990; Drummond and Defant, 1990). The major element definition is provided by high pressure and temperature experiments on the partial melting of amphibolite-grade metamorphosed basalt (Beard and Lofgren, 1991; Rapp et al., 1991; Rushmer, 1991; Sen and Dunn, 1994; Wolf and Wyllie, 1994; Rapp and Watson, 1995; Lopez and Castro, 2001). Broad distinguishing characteristics include $SiO_2 > 56$ wt.% and “trondhjemitic” affinities (high Na/K, Barker, 1979), which serve to distinguish amphibolite melts from peridotite melts (which typically have $SiO_2 < 50\%$), and melts of pelites (which are “granitic,” i.e., higher in K_2O). The adakitic trace element signature is defined by a high Sr, Sr/Y, La/Yb, and low Y and Yb, consistent with the *presence* of garnet (to account for low Y, Yb and high La/Yb values) and the *absence* of plagioclase (to account for the high Sr contents and Sr/Y and the absence of an Eu anomaly) in the same rock. The Mg#, and Ni and Cr contents of pure slab melts should be low (e.g., Mg#<40; (Sen and Dunn, 1994; Rapp and Watson, 1995). However, the observed abundances in rocks interpreted to be, at least in part, slab melts are much higher. The high-Mg# and compatible element contents of putative slab melts are typically attributed to reaction between ascending silicic melts and mantle peridotite after partial melting of subducted crust (Kay, 1978; Rapp et al., 1999).

Adakitic magmas can be generated by means other than slab melting. Atherton and Petford (1993) identified adakites in the Cordillera Blanca batholith of Peru that they interpreted to be the result of melting of underplated basalt at the base of

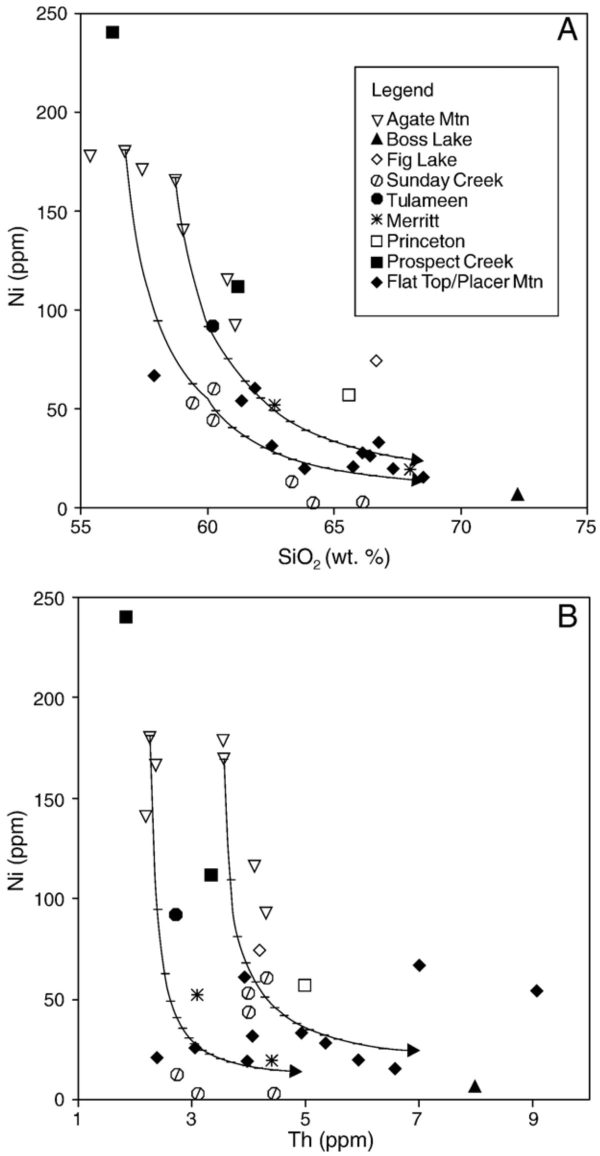

Fig. 11. Raleigh-type fractional crystallization modelling. The two lines represent modelled liquid-lines-of-descent from two different parental compositions (RBI-04-16-14-1; RBI-04-15-13-1). Each model has two stages. Olivine + clinopyroxene + magnetite are fractionated until the magma is at 60 wt.% SiO_2, then hornblende + plagioclase + apatite + zircon + magnetite are fractionated. Tic marks represent 2% crystallization increments.

continental crust. Feeley and Hacker (1995) studied a Quaternary stratovolcano in the Central Volcanic Zone of the Andes and concluded that adakites at this volcanic centre were derived though the interaction of basaltic magmas with garnet-bearing rocks at the base of the crust, and assimilation, followed by low pressure fractional crystallization to produce andesites and dacites. Other hypotheses on the origin of specific adakites include delamination of basaltic crust (Xu et al., 2002; Gao et al., 2004), subduction erosion (Kay and Kay, 2002), magma mixing (Streck et al., 2007) and remelting of arc basalt trapped and solidified in the upper mantle (Macpherson and Hall, 2002).

7.2. Adakites in the Princeton Group: petrogenesis of primitive magmas

The least evolved high-Mg# andesites in the Princeton Group best record information on the nature of the mantle source area and the melt regime as they have been least modified by processes such as crystal fractionation or assimilation of crustal material. The most primitive suite of volcanic rocks in the Princeton Group is the olivine+clinopyroxene+opaque basaltic andesites and andesites exposed at and within a few km of Agate Mountain. A lone sample from Prospect Creek has a higher MgO at 9.2% but has little stratigraphic context and will not be considered in further detail. Three of these samples are in Fe–Mg equilibrium with Fo_{88-89} olivine a composition near to that of typical mantle olivine ($\geq Fo_{90}$). Although they are not adakites *sensu-stricto* (because of slightly lower SiO_2 or Al_2O_3 than permitted in the definition) they have "adakitic" trace element signatures such as fractionated REE (La/Yb=16–34), fractionated and low HREE (Gd/Yb=3.2–4.6) and high Sr/Y (90–145). In addition they have very high LILE contents, including Ba>690 ppm and Sr>985 pm.

Two hypotheses are explored below using trace element modelling. One is the mainstream adakite hypothesis, i.e., that the adakitic high-Mg# andesites formed by the melting of subducted and metamorphosed oceanic crust and evolved by melt–rock reaction with mantle peridotite. For this model, an average NMORB from the East Pacific Rise (determined using the PETDB compilation; http://www.petdb.org) is used as the composition of the subducted slab. The second hypothesis is that they were generated by melting of metabasalt with arc-like (rather than MORB-like) trace element abundances. For this model, arc basalts from the Cretaceous Spences Bridge Group (Smith and Thorkelson, 2002) and Triassic Nicola Group (Mortimer, 1987) were selected. Both the Nicola and Spences Bridge groups are basement to the Princeton Group.

7.3. Trace element modelling

The model concentrations of Ba, Th, Nb, La, Sr, Zr, Sm, Gd, Y, and Yb were calculated at 15–25% batch partial melting, with 49.5% garnet and clinopyroxene and 1% rutile, with and without the addition of small amounts (<5%) of plagioclase and hornblende, followed by reaction with peridotite (Fig. 12). The modes were estimated from the experimental studies of Rapp and Watson (1995) and Sen and Dunn (1994). Silicic melt–peridotite reaction is dominated by the dissolution of olivine and precipitation of orthopyroxene and possibly garnet, the effect of which on incompatible trace elements is primarily dilution (Rapp et al., 1999). Melt–peridotite reaction has a negligible effect on the incompatible trace element ratios of the melt, for example Sr/Y, La/Yb, Sr/Zr, or La/Ba (Rapp et al., 1999). The

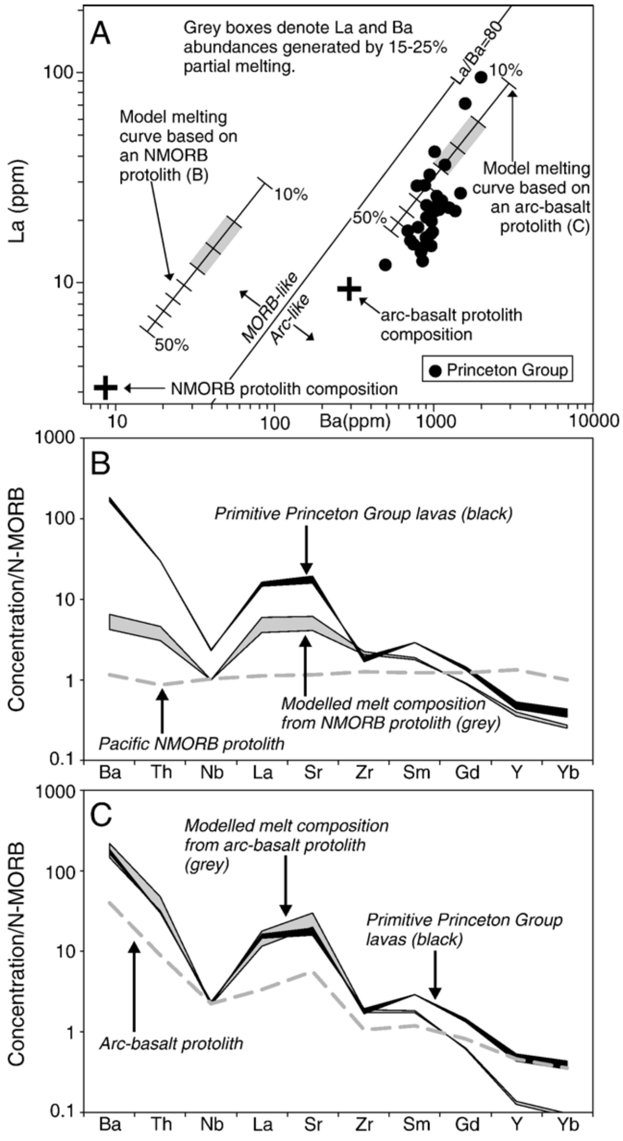

Fig. 12. The results of modeling trace element behavior during partial melting of garnet–amphibolite in the upper mantle. Two different model melt composition were calculated for two different starting compositions, one resembling Pacific NMORB and the other resembling an arc basalt. The results of both models are depicted here. A) Ba vs. La diagram illustrating that an NMORB starting composition poorly reproduces both the Ba and La abundances and the Ba–La ratio (all samples from the Princeton Group are depicted), whereas an arc-like starting composition provides a much better fit to the data. Barium and La abundances are poorly fractionated during partial melting and Ba–La ratios largely retain the value of their source. Line dividing arc-like La/Ba from MORB-like La/Ba from Gill (1981). Tics are 5% partial melting. B) The results of the model using a Pacific NMORB starting composition. The starting composition is dashed and the preferred range of modeled values is in grey. For comparison, the range of values in two adakitic, primitive, Princeton Group lavas are shown. C) The results of the model using an arc basalt starting composition. NMORB normalizing values from Sun and McDonough (1989).

amount of dilution required to bring an amphibolite–melt to Fe–Mg equilibrium with mantle olivine (~Fo_{90}) is 10–15% (Stern and Kilian, 1996).

Sets of mineral/melt partition coefficients at relevant pressures, temperatures, and compositions are used. Partitioning data for hydrous, tonalitic melts at 18 kb and 1000–1040 °C, (Barth et al., 2002), have been used for garnet and clinopyroxene with the exception of the Th partition coefficient, which was taken from Klemme et al. (2002). Partition coefficients for hornblende were from the 2–5 kb, 900–945 °C experiments of Hilyard et al. (2000) on hydrous, dacitic melts with the exception of Ba from Brenan et al. (1995) and Th, estimated from the GERM database (Geochemical Earth Reference Model; http://www.earthref.org/). Rutile partition coefficients are currently poorly understood, but those from Foley et al. (2000) compare well with those of Xiong et al. (2005) and are used herein. Plagioclase partition coefficients were calculated by the method of Wood and Blundy (2003) using An_{60} and 950 °C with the exception of Nb, which was estimated from the GERM database and Th, which was assumed to be identical to U (Wood and Blundy, 2003).

The modelled melt composition is insensitive to modest changes in the abundances of residual clinopyroxene and garnet, (for example by changing garnet or clinopyroxene to as much as 75% of the total mode) and the addition of small amounts of hornblende (up to 15%). It is highly sensitive to changes in the amount of rutile and plagioclase, which dominate the Nb and Sr budgets, respectively.

7.4. Results of trace element modelling

Using the trace element concentrations of NMORB as the magma source composition yields a model composition that poorly matches those of high-Mg# andesites in the Princeton Group (Fig. 12). In particular, the model melt has abundances of the LILE and LREE, and ratios of La/Yb, Sr/Y, Ba/La which are well below those of the Princeton andesites, although they approximately match the Princeton samples in Nb, Zr, Y and Yb concentrations.

Using Spences Bridge Group arc basalt as the composition of the magma source provides a much better fit to most of the observed trace element abundances. The resultant melts match the Princeton Group andesites in all modelled elements, except for the HREE and Y, which are much lower in the modelled compositions (~0.3 ppm Yb in the model vs. ~1 ppm Yb in the observed rocks). The discrepancy is the result of low concentrations of the HREE in the Spences Bridge Group (relative to many arc basalts), which may have been caused by interaction of Spences Bridge Group basalt with garnet at the base of the crust, or mixing with slab-anatectic melts (Smith and Thorkelson, 2002). The modelled HREE concentrations are extremely low compared to typical crustal rocks but comparable to those in mantle peridotite (Rudnick and Gao, 2003; Canil, 2004). Such low concentrations are highly vulnerable to change by very small degrees of contamination from the crust. The discrepancy is likely due to either a small degree of contamination (extremely low trace element concentrations are vulnerable to small amounts of crustal contamination) or the use of an inappropriate protolith. Using an averaged Triassic basalt from the Nicola Group (Mortimer, 1987) as the magma source also yields a melt composition that closely matches the Princeton Group. The fit is slightly better in the HREE, but slightly poorer in the LILE, relative to the Spences Bridge Group model. Using either of the Mesozoic arc basalts yields a better overall fit than by using an NMORB source.

7.5. Petrogenesis

The trace element modelling and phase relations place important constraints on the origin of primitive, adakitic high-Mg# andesites in the Princeton Group. The compositions of these rocks are consistent with a two-stage process: 1) Partial melting of basaltic rocks with primitive arc-like trace element compositions at depths of approximately 30–80 km (e.g., Fig. 13) and, 2)

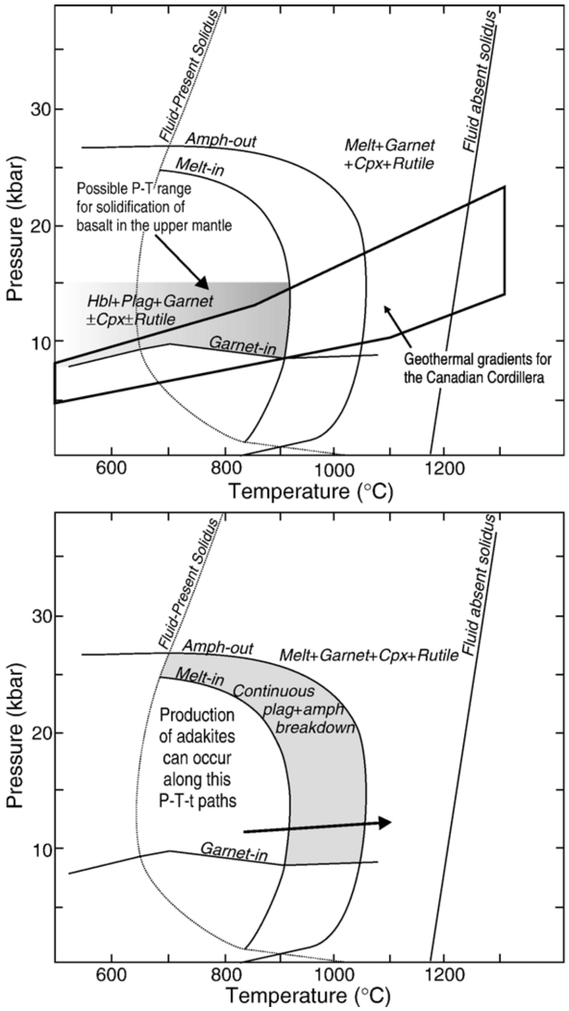

Fig. 13. Depiction of important phase relations in the generation of adakites in the lithospheric mantle. Phase relationships are after Vielzeuf and Schmidt (2001), with additions to the hornblende-out curve after Rapp (1995) and Sen and Dunn (1994). A) Region of stability of solid basalt (amphibolite) in *P–T* space for the upper mantle. The shaded areas are the geothermal gradients for the crust and upper mantle of high-heat flow orogens (after Lewis et al., 2003, as discussed in text). B) Possible *P–T–t* path that would form adakitic magmas from amphibolite in the upper mantle (arrow).

reaction of the amphibolite-derived melt with peridotite, leading to elevation of Mg# and compatible element concentrations, and possibly enrichment in HREE (Fig. 14). This process can only occur where melting of meta-basalt occurs in the mantle environment.

A number of mechanisms are capable of introducing arc basalt into the lithospheric mantle. Delamination (Kay and Kay, 1993) or convective "dripping" (Jull and Kelemen, 2001) of mafic, garnet-bearing, high density crustal rocks into the mantle has been proposed by Gao et al. (2004) and Xu et al. (2002) for the generation of adakites in China. In these models, the heating of the detached crustal blocks leads to adakite melt generation; the melts become increasingly mafic by reaction with mantle peridotite during their ascent. This scenario, however, may be unlikely for genesis of the Princeton Group because it seems to require wholesale removal of lithospheric mantle along with the lower crust (Kay and Kay, 1993; Lustrino, 2005). This is incompatible with studies of mantle xenoliths which identify that ancient lithospheric mantle is preserved through the Canadian Cordillera until at least late-Tertiary time (Peslier et al., 2000), additionally the Chinese adakites occur in an intraplate setting in contrast to the active margin setting of the Princeton Group. Jull and Kelemen (2001), however, have calculated that convective instabilities between the crust and lithospheric mantle are possible and could result in foundering of lower crust without the loss of lithospheric mantle. If so, this hypothesis is difficult to rule out.

A second mechanism is subduction erosion (Kay and Kay, 2002; von Huene et al., 2004) in which a subducting slab drags ancient arc volcanic rocks from the forearc (for example, rocks presently preserved on Vancouver Island and the Queen Charlotte Islands) into the subduction zone. As proposed by Kay and Kay (2002), these blocks would be dragged by corner flow along with the subducted slab into deeper and hotter parts of the mantle, where they would melt. In this model, however, the melting of entrained blocks would likely be accompanied by partial melting of oceanic crust for which there is no geochemical evidence.

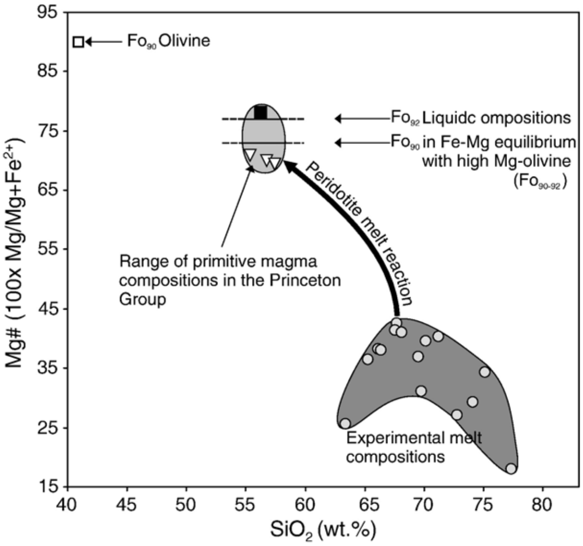

Fig. 14. Diagram illustrating the chemical evolution of a silicic partial melt in the mantle. A partial melt of garnet amphibolite interacts with peridotite, dissolving olivine and precipitating a small amount of pyroxene (e.g., Stern and Kilian, 1996; Rapp et al., 1999). The primary effect is to increase the Mg# of the melt and increase concentrations of compatible elements (e.g., Ni and Cr). The maximum Mg# that the melt can likely reach is defined by Mg–Fe equilibria between high-Mg, mantle olivine and melt (e.g., Roeder and Emslie, 1970), shown by horizontal lines. Experimental compositions from Rapp and Watson (1995) and Sen and Dunn (1994).

In a third mechanism, arc basalt was emplaced into the lithospheric mantle as dikes and sills during previous intervals of arc magmatism (e.g., Macpherson and Hall, 2002; Melcher and Meisel, 2004), and these intrusions were then partially melted during re-heating of the lithospheric mantle in the Eocene. Such intrusions could have originally been emplaced as feeder dykes to the Nicola and Spences Bridge groups. This scenario requires that the temperature of the lithospheric mantle in the Mesozoic was below the wet basalt solidus so that the mafic dykes would completely solidify. The temperature of the lithosphere was probably no hotter than that proposed by Lewis et al. (2003; see also Harder and Russell, 2006) for the modern Canadian Cordillera, which is considered to be representative of hot orogenic belts throughout the world (Hyndman et al., 2005). Using their geothermal gradients and a wet basalt solidus of approximately 900 °C (Fig. 13), the temperature of the lithospheric mantle would be cold enough to induce crystallization in dykes of arc basalt at depths <45 km (Fig. 13). Subsequent heating of the lithospheric mantle would cause partial melting of these dykes, yielding adakitic magmas. These melts would react with the surrounding peridotite and would become increasingly mafic, with higher Mg#, Ni and Cr, and rise into the crust as adakitic high-Mg# andesites (Fig. 14).

The melting of intrusions of LILE- and LREE-enriched arc basalt that were previously emplaced into the lithospheric mantle is our preferred hypothesis for generating primitive andesites in the Princeton Group. It is difficult to exclude subduction erosion and delamination for the Princeton Group itself, but neither mechanism can explain volcanic activity throughout the entire belt, where a similar age, style, and chemistry of volcanic activity imply a broadly similar trigger. This conclusion is consistent with those of a number of workers who, largely on isotopic grounds, identified the melting of enriched lithospheric mantle in the central and southernmost parts of the Challis–Kamloops belt. These volcanic fields include the Penticton Group (Dostal et al., 2003), the Colville Igneous Complex (Morris et al., 2000), the Challis Group (McKervey, 1998), the Absaroka Supergroup (Feeley, 2003), the Buck Creek Complex (Dostal et al., 2001), and the Montana Alkalic Province (Dudas, 1991). The origin of coeval volcanic rocks to the north, including the Buck Creek Complex, the Endako Group, the Ootsa Lake Group, and the Clisbako volcanics is less clear, although Dostal et al. (2001) suggested that volcanic activity in the Buck Creek complex (Fig. 1) could have involved anatexis of lithospheric mantle.

7.6. Tectonic setting of the Princeton Group

Asthenospheric upwelling has been proposed by a number of workers as a trigger for anatexis of lithospheric mantle in the

Challis–Kamloops belt, and is herein regarded as the most likely cause of Princeton Group magmatism. The cause of the upwelling is uncertain, but two plate tectonic mechanisms have been proposed. In one, the asthenosphere welled up through a slab window emanating from a ridge-trench intersection somewhere along the Oregon–British Columbia coast (Thorkelson and Taylor, 1989; Breitsprecher et al., 2003; Haeussler et al., 2003). A slab window is a slab-free region underneath an overriding plate that develops as a consequence of a ridge-trench intersection (Dickinson and Snyder, 1979; Thorkelson, 1996; Sisson et al., 2003). The presence of an Eocene slab window underneath British Columbia and the northwestern United States would replace cool, subducted oceanic lithosphere and the refrigerated mantle wedge with hot, sub-slab asthenosphere (Thorkelson, 1996; Johnston and Thorkelson, 1997). Magnetic anomalies preserved on the sea-floor in the Gulf of Alaska provide evidence for two oceanic plates, the Farallon and the Kula, subducting underneath North America during the early Tertiary. In addition, a growing wealth of onshore geological data seems to require the presence of at least one additional plate in the north Pacific region in the early Tertiary, i.e., the Resurrection plate of Haeussler et al. (2003). Madsen et al. (2006) further demonstrated the need for the Resurrection plate, but argued for its eventual separation into two sub-plates, the more northern of which they named the Eshamy plate. Thus, the most recent plate models show a complex pattern of slab windows among the subducted slabs of the Farallon, Kula, Resurrection and possibly Eshamy plates beneath the northern Cordillera during the early Tertiary. These complex patterns would have had a large influence of the thermal state of the upper mantle beneath western North America at the time, and contributed to widespread lithospheric

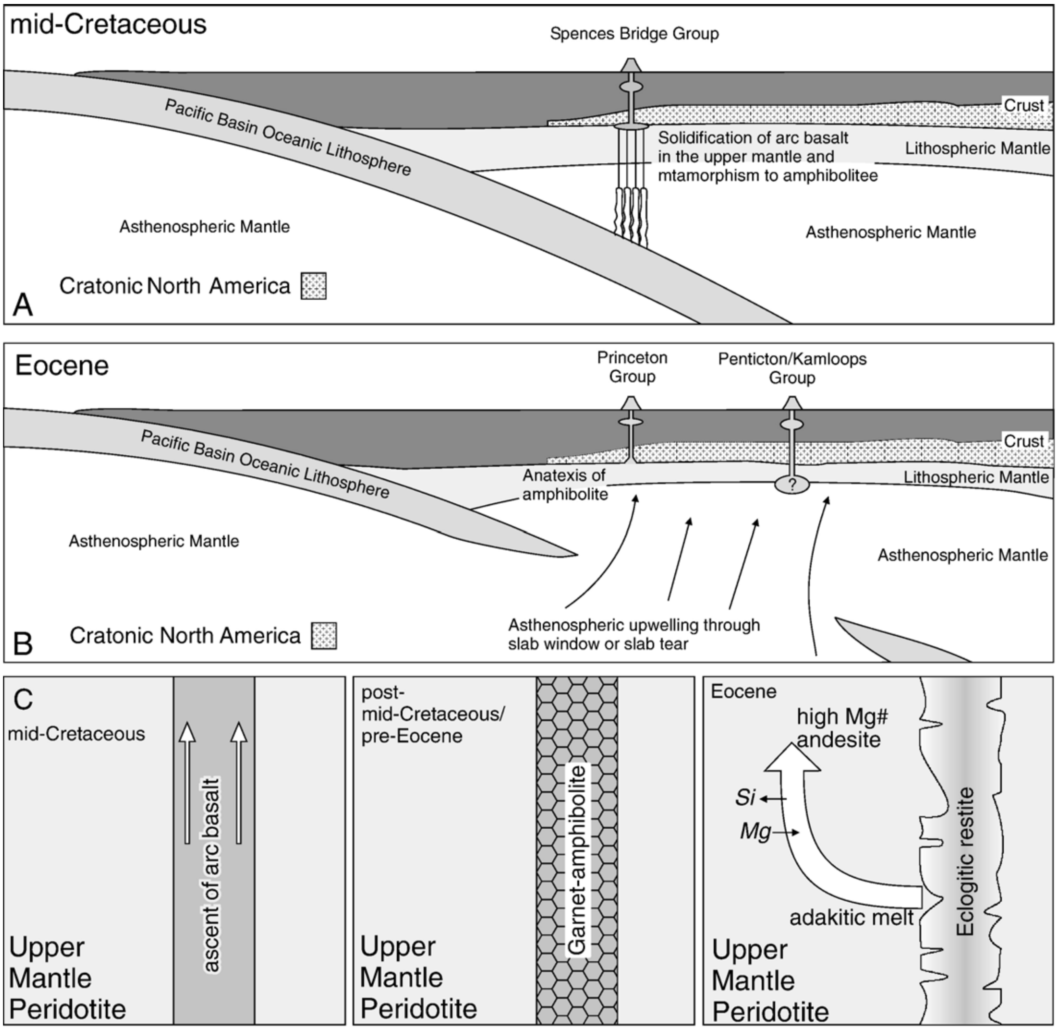

Fig. 15. Diagram illustrating the preferred mechanism for the genesis of the Princeton Group and related Challis–Kamloops volcanic fields. A) Arc volcanism in the Mesozoic (Spences Bridge Group represented in this case) emplaces arc basalt in the upper mantle. Dikes from previous episodes of magmatism, for example the Triassic Nicola Group, may already have been emplaced. B) Upwelling of asthenosphere, either through a slab window or a slab tear, heats the lithospheric mantle. In the case of the Princeton Group, heterogeneities of Mesozoic arc basalt in the lithospheric mantle are partially melted, and the resultant adakitic magmas interact with mantle peridotite to form high-Mg# andesite with adakitic trace element signature. Elsewhere in the Challis–Kamloops field, heating is more extensive and along with lithospheric mantle, melting of the asthenosphere is also likely. The approximate location of cratonic North American crust is from Clowes et al. (1995). C) Schematic diagram of the evolution of a hypothetical basaltic dike from inception as a feeder to a Mesozoic arc, to solidifying into amphibolite, to partial melting and reacting with ambient peridotite during the Eocene thermal event.

heating. These tectonic and magmatic processes are illustrated in Fig. 15.

Other workers have proposed an alternative, where magmatism was triggered by breaking off of low-angle or “flat” subducted oceanic lithosphere of the Farallon plate (Humphreys, 1995; McKervey, 1998; Feeley, 2003). Foundering of the broken part of the slab would permit influx of hot asthenosphere, triggering melting in the lithospheric mantle. This model accounts well for the late-Tertiary “sweep” of magmatism across the United States (Humphreys, 1995), although it has not been explicitly applied to magmatic activity to the north, in Canada. If slab break-off were the cause of the lithospheric heating, then it would have had to occur nearly simultaneously for an along-strike distance of >1000 km, i.e., from beneath the western United States through central British Columbia, implying the existence of a single subducted slab at that time, or the fortuitous tearing-away of more than one plate. As noted earlier, offshore and onshore geological records suggest that at least two additional plates were subducting beneath the region, and that continuity of a single slab beneath that stretch of the Cordillera in Eocene time is unlikely.

8. Conclusions

The Princeton Group of south-central British Columbia is part of the Eocene Challis–Kamloops magmatic belt which extends from northern British Columbia to the western United States. The group consists of calc–alkaline volcanic and terrestrial sedimentary rocks that were deposited in a regime of dextral transtension. The volcanic rocks accumulated as cinder cones and stratovolcanoes, partly within extensional basins. New geochronological results indicate that they were erupted from approximately 53–47 Ma, similar to the interval of magmatism in other Challis–Kamloops successions.

Princeton Group lavas range from basaltic andesite to rhyolite, and differentiated by fractional crystallization with subordinate magma mixing and assimilation. Most have unusually primitive characteristics for rocks with $SiO_2 > 55$ wt.% (including high-Mg#, Ni and Cr contents) and are classified as high-Mg# andesites. An adakitic geochemical signature is present at the full range of rock compositions, including the high-Mg# andesites. Major and trace element abundances of the most primitive lavas are consistent with genesis by high-pressure anatexis of meta-basalt with arc-like trace element systematics, followed by reaction with mantle peridotite. Melting of a subducted slab with an NMORB composition (a commonly invoked method of producing adakite) is incapable of producing the observed high LILE abundances in the Princeton Group. As well, anatexis of lower crustal rocks of the North American plate is not viable because the resulting melts would be unable to react with mantle peridotite, and would therefore remain more felsic than the high-Mg# andesites of the Princeton Group.

The most likely scenario for the origin of the primitive Princeton Group rocks involves Eocene heating of North American lithospheric mantle containing dykes of arc basalt which were emplaced during an earlier event of arc magmatism. At least two pre-Eocene events of arc magmatism in the area, represented by the Triassic Nicola Group and the Cretaceous Spences Bridge Group, could have contributed to this intrusive event. The most likely cause of lithospheric heating is the upwelling of hot asthenosphere, probably through a geometrically complex set of slab windows that developed as a result of microplate formation along the western margin of North America during the early Tertiary (e.g., Haeussler et al., 2003; Madsen et al., 2006). Alternatively, upwelling may have been induced through the break-off and foundering of low-angle subducted lithosphere, or by a combination of the two processes.

Acknowledgements

DJT is supported by a grant from the Natural Sciences and Engineering Research Council of Canada (NSERC). RBI was supported by a NSERC post-graduate scholarship and a Simon Fraser University entrance scholarship. RBI thanks Christa Sluggett and Dejan Milidragovic for field assistance, and James Scoates and Dominique Weis for Nd isotope measurements. Kelly Russell, James Scoates and Dante Canil are thanked for comments on an earlier version of this manuscript.

Appendix A. Supplementary data

Supplementary data associated with this article can be found, in the online version, at doi:10.1016/j.tecto.2007.10.007.

References

Atherton, M.P., Petford, N., 1993. Generation of sodium-rich magmas from newly underplated basaltic crust. Nature 362 (6416), 144–146.

Bardoux, 1993. The Okanagan Valley normal fault from Penticton to Enderby, south-central British Columbia. PhD Thesis, Carleton University, Ottawa, 292 pp.

Barker, F., 1979. Trondhjemite: definition, environment and hypotheses of origin. In: Barker, F. (Ed.), Trondhjemites, Dacites, and Related Rocks. Elsevier, New York, pp. 1–12.

Barth, M.G., Foley, S.F., Horn, I., 2002. Partial melting in Archean subduction zones: constraints from experimentally determined trace element partition coefficients between eclogitic minerals and tonalitic melts under upper mantle conditions. Precambrian Research 113 (3–4), 323–340.

Beard, J.S., Lofgren, G.E., 1991. Dehydration melting and water-saturated melting of basaltic and andesitic greenstones and amphibolites at 1, 3, and 6.9 kb. Journal of Petrology 32 (2), 365–401.

Breitsprecher, K., 2002. Volcanic stratigraphy, petrology and tectonic setting of the eastern margin of the Eocene Kamloops Group, south-central British Columbia. M.Sc. Thesis, Simon Fraser University, Burnaby, 221 pp.

Breitsprecher, K., Thorkelson, D.J., Groome, W.G., Dostal, J., 2003. Geochemical confirmation of the Kula–Farallon slab window beneath the Pacific Northwest in Eocene time. Geology 31 (4), 351–354.

Brenan, J.M., Shaw, H.F., Ryerson, F.J., Phinney, D.L., 1995. Experimental determination of trace-element partitioning between pargasite and a synthetic hydrous andesitic melt. Earth and Planetary Science Letters 135 (1–4), 1–11.

Burchfiel, B.C., 1993. Tectonostratigraphic map of the Cordilleran orogenic belt: contimerous United States. In: Burchfiel, B.C., Lipman, P.W., Zoback, M.L. (Eds.), The Cordilleran Orogen: Conterminous U.S. Geological Society of America, Boulder, Colorado.

Camsell, C., 1913. Geology and Mineral Deposits of the Tulameen District, B.C. Memoir 26. Geological Survey of Canada.

Canil, D., 2004. Mildly incompatible elements in peridotites and the origins of mantle lithosphere. Lithos 77 (1–4), 375–393.

Church, B.N., 1973. Geology of the White Lake Basin. Bulletin, vol. 61. British Columbia Department of Mines and Petroleum Resources, Victoria, BC.

Church, B.N., 1979. Tertiary stratigraphy and resource potential in south-central British Columbia (82E, L). Geological Fieldwork 1978, Paper 1979-1. British Columbia Ministry of Energy, Mines and Petroleum Resources, Victoria, BC.

Church, B.N., Suesser, U., 1983. Geology and magnetostratigraphy of Miocene basalts of the Okanagan Highlands, British Columbia (82L/2,3). Geological Fieldwork 1982, Paper 1983-1. British Columbia Ministry of Energy, Mines and Petroleum Resources, Victoria, BC.

Clowes, R.M., Zelt, C.A., Amor, J.R., Ellis, R.M., 1995. Lithospheric structure in the southern Canadian Cordillera from a network of seismic refraction lines. Canadian Journal of Earth Sciences 32 (10), 1485–1513.

De Paolo, D.J., 1981. Trace-element and isotopic effects of combined wallrock assimilation and fractional crystallization. Earth and Planetary Science Letters 53 (2), 189–202.

Defant, M.J., Drummond, M.S., 1990. Derivation of some modern arc magmas by melting of young subducted lithosphere. Nature 347 (6294), 662–665.

Defant, M.J., Kepezhinskas, P., 2001. Evidence suggests slab melting in arc magmas. Eos, Transactions of the American Geophysical Union 82, 65–69.

Dickinson, W.R., 1991. Tectonic setting of faulted Tertiary strata associated with the Catalina core complex in southern Arizona. GSA Special paper, vol. 264. Geological Society of America. 106 pp.

Dickinson, W.R., 2004. Evolution of the North American Cordillera. Annual Review of Earth and Planetary Sciences 32, 13–45.

Dickinson, W.R., Snyder, W.S., 1979. Geometry of triple junctions related to San Andreas transform. Journal of Geophysical Research 84 (NB2), 561–572.

Dostal, J., Church, B.N., Reynolds, P.H., Hopkinson, L., 2001. Eocene volcanism in the Buck Creek basin, central British Columbia (Canada): transition from arc to extensional volcanism. Journal of Volcanology and Geothermal Research 107 (1–3), 149–170.

Dostal, J., Breitsprecher, K., Church, B.N., Thorkelson, D., Hamilton, T.S., 2003. Eocene melting of Precambrian lithospheric mantle: analcime-bearing volcanic rocks from the Challis–Kamloops belt of south central British Columbia. Journal of Volcanology and Geothermal Research 126 (3–4), 303–326.

Dostal, J., Owen, J.V., Church, B.N., Hamilton, T.S., 2005. Episodic volcanism in the Buck Creek complex (Central British Columbia, Canada): a history of magmatism and mantle evolution from the Jurassic to the early Tertiary. International Geology Review 47 (6), 551–572.

Drummond, M.S., Defant, M.J., 1990. A model for trondhjemite–tonalite–dacite genesis and crustal growth via slab melting-Archean to modern comparisons. Journal of Geophysical Research-Solid Earth and Planets 95 (B13), 21503–21521.

Dudas, F.O., 1991. Geochemistry of igneous rocks from the Crazy Mountains, Montana, and tectonic models for the Montana Alkalic Province. Journal of Geophysical Research-Solid Earth and Planets 96 (B8), 13261–13277.

Eisele, J., et al., 2002. The role of sediment recycling in EM-1 inferred from Os, Pb, Hf, Nd, Sr isotope and trace element systematics of the Pitcairn hotspot. Earth and Planetary Science Letters 196–212 (3–4), 197.

Ewing, T.E., 1980. Paleogene tectonic evolution of the Pacific Northwest. The Journal of Geology 88 (6), 619–638.

Ewing, T.E., 1981a. Petrology and geochemistry of the Kamloops Group, British Columbia. Canadian Journal of Earth Sciences 18, 1478–1491.

Ewing, T.E., 1981b. Regional stratigraphy and structural setting of the Kamloops Group, south-central British Columbia. Canadian Journal of Earth Sciences 18, 1464–1477.

Feeley, T.C., 2003. Origin and tectonic implications of across-strike geochemical variations in the Eocene Absaroka volcanic province, United States. Journal of Geology 111 (3), 329–346.

Feeley, T.C., Cosca, M.A., 2003. Time vs. composition trends of magmatism at Sunlight volcano, Absaroka volcanic province, Wyoming. Geological Society of America Bulletin 115 (6), 714–728.

Feeley, T.C., Hacker, M.D., 1995. Intracrustal derivation of Na-rich andesitic and dacitic magmas — an example from Volcan Ollague, Andean Central Volcanic Zone. Journal of Geology 103 (2), 213–225.

Feeley, T.C., Cosca, M.A., Lindsay, C.R., 2002. Petrogenesis and implications of calc–alkaline cryptic hybrid magmas from Washburn volcano, Absaroka Volcanic Province, USA. Journal of Petrology 43 (4), 663–703.

Foley, S.F., Barth, M.G., Jenner, G.A., 2000. Rutile/melt partition coefficients for trace elements and an assessment of the influence of rutile on the trace element characteristics of subduction zone magmas. Geochimica et Cosmochimica Acta 64 (5), 933–938.

Gao, S., et al., 2004. Recycling lower continental crust in the North China craton. Nature 432 (7019), 892–897.

Garrison, J.M., Davidson, J.P., 2003. Dubious case for slab melting in the Northern volcanic zone of the Andes. Geology 31 (6), 565–568.

Ghosh, D.K., 1995. Nd–Sr isotopic constraints on the interactions of the Intermontane Superterrane with the western edge of North America in the southern Canadian Cordillera. Canadian Journal of Earth Sciences 32 (10), 1740–1758.

Gill, J., 1981. Orogenic Andesites and Plate Tectonics. Springer, Berlin. 336 pp.

Goldstein, S.L., Onions, R.K., Hamilton, P.J., 1984. A Sm–Nd isotopic study of atmospheric dusts and particulates from major river systems. Earth and Planetary Science Letters 70 (2), 221–236.

Grainger, N.C., Villeneuve, M.E., Heaman, L.M., Anderson, R.G., 2001. New U–Pb and Ar/Ar isotopic age constraints on the timing of Eocene magmatism, Fort Fraser and Nechako River map areas, central British Columbia. Canadian Journal of Earth Sciences 38 (4), 679–696.

Grove, T.L., Parman, S.W., Bowring, S.A., Price, R.C., Baker, M.B., 2002. The role of an H_2O-rich fluid component in the generation of primitive basaltic andesites and andesites from the Mt. Shasta region, N California. Contributions to Mineralogy and Petrology 142 (4), 375–396.

Haeussler, P.J., Bradley, D.C., Wells, R.E., Miller, M.L., 2003. Life and death of the Resurrection plate: evidence for its existence and subduction in the northeastern Pacific in Paleocene–Eocene time. Geological Society of America Bulletin 115 (7), 867–880.

Harder, M., Russell, J.K., 2006. Thermal state of the upper mantle beneath the Northern Cordilleran Volcanic Province (NCVP), British Columbia, Canada. Lithos 87 (1–2), 1–22.

Hilyard, M., Nielsen, R.L., Beard, J.S., Patino Douce, A.E., Blencoe, J., 2000. Experimental determination of the partitioning behavior of rare earth and high field strength elements between pargasitic amphibole and natural silicate melts. Geochimica et Cosmochimica Acta 64 (6), 1103–1120.

Hiza, M., 1999. The geochemistry and geochronology of the Eocene Absaroka volcanic province, northern Wyoming and southwest Montana, United States of America. PhD Thesis, Oregon State University, 243 pp.

Hofmann, A.W., 2003. Sampling mantle heterogeneity through oceanic basalts: isotopes and trace elements. In: Rudnick, R.L. (Ed.), The Crust. Treatise on Geochemistry. Elsevier, pp. 64–101.

Humphreys, E.D., 1995. Post-Laramide removal of the Farallon slab, western United-States. Geology 23 (11), 987–990.

Hunt, P.A., Roddick, J.C., 1990. A compilation of K–Ar ages: report 19. Radiogenic Age and Isotopic Studies: Report 3. Paper 87-2, Geological Survey of Canada Paper 89-2.

Hyndman, R.D., Currie, C.A., Mazzotti, S.P., 2005. Subduction zone backarcs mobile belts, and orogenic heat. GSA Today 15 (2), 4–10.

Ickert, R.B., 2006. Adakitic Volcanism in Southern BC During the Early Eocene: Isotopic and Geochemical Constraints from the Princeton Group. Simon Fraser University, Burnaby, BC. 105 pp.

Irvine, T.N., Baragar, W.R.A., 1971. Guide to chemical classification of common volcanic rocks. Canadian Journal of Earth Sciences 8 (5), 523–548.

Janecke, S.U., Snee, L.W., 1993. Timing and episodicity of Middle Eocene volcanism and onset of conglomerate deposition, Idaho. Journal of Geology 101 (5), 603–621.

Janecke, S.U., Hammond, B.F., Snee, L.W., Geissman, J.W., 1997. Rapid extension in an Eocene volcanic arc: structure and paleogeography of an intra-arc half graben in central Idaho. Geological Society of America Bulletin 109 (3), 253–267.

Johnston, S.T., Thorkelson, D.J., 1997. Cocos–Nazca slab window beneath Central America. Earth and Planetary Science Letters 146 (3–4), 465–474.

Jull, M., Kelemen, P.B., 2001. On the conditions for lower crustal convective instability. Journal of Geophysical Research-Solid Earth 106 (B4), 6423–6446.

Kay, R.W., 1978. Aleutian magnesian andesites: melts from subducted Pacific Ocean crust. Journal of Volcanology and Geothermal Research 4, 497–522.

Kay, R.W., Kay, S.M., 1993. Delamination and delamination magmatism. Tectonophysics 219 (1–3), 177–189.

Kay, R.W., Kay, S.M., 2002. Andean adakites: three ways to make them. Acta Petrologica Sinica 18 (3), 303–311.

Kelemen, P.B., 1995. Genesis of high Mg-number andesites and the continental-crust. Contributions to Mineralogy and Petrology 120 (1), 1–19.

Kelemen, P.B., Hanghoj, K., Greene, A.R., 2003. One view of the geochemistry of subduction-related magmatic arcs, with an emphasis on primitive andesite and lower crust. In: Rudnick, R.L. (Ed.), The Crust. Treatise on Geochemistry. Elsevier, pp. 594–649.

Klemme, S., Blundy, J.D., Wood, B.J., 2002. Experimental constraints on major and trace element partitioning during partial melting of eclogite. Geochimica et Cosmochimica Acta 66 (17), 3109–3123.

Le Maitre, R.W. (Ed.), 2002. Igneous Rocks, A Classification and Glossary of Terms. Cambridge University Press, Cambridge. 236 pp.

Lewis, T.J., Hyndman, R.D., Fluck, P., 2003. Heat flow, heat generation, and crustal temperatures in the northern Canadian Cordillera: thermal control of tectonics. Journal of Geophysical Research-Solid Earth 108 (B6).

Lindsay, C.R., Feeley, T.C., 2003. Magmagenesis at the Eocene Electric Peak-Sepulcher Mountain complex, Absaroka Volcanic Province, USA. Lithos 67 (1–2), 53–76.

Lopez, S., Castro, A., 2001. Determination of the fluid-absent solidus and supersolidus phase relationships of MORB-derived amphibolites in the range 4–14 kbar. American Mineralogist 86 (11–12), 1396–1403.

Ludwig, K.R., 2003. Isoplot 3.09 A Geochronological toolkit for Microsoft Excel., Berkeley Geochronology Center. Special Publication No. 4.

Lustrino, M., 2005. How the delamination and detachment of lower crust can influence basaltic magmatism. Earth-Science Reviews 72 (1–2), 21–38.

Macpherson, C.G., Hall, R., 2002. Timing and tectonic controls in the evolving orogen of SE Asia and the western Pacific and some implications for ore generation. In: Blundell, D.J., Neubauer, F., von Quadt, A. (Eds.), The Timing and Location of Major Ore Deposits in an Evolving Orogen. Geological Society, London, pp. 49–67.

Madsen, J.K., Thorkelson, D.J., Friedman, R.M., Marshall, D.D., 2006. Cenozoic to Recent plate configurations in the Pacific Basin: ridge subduction and slab window magmatism in western North America. Geosphere 2 (1), 11–34.

Martin, H., 1999. Adakitic magmas: modern analogues of Archaean granitoids. Lithos 46 (3), 411–429.

Massey, N.W.D., MacIntyre, D.G., Desjardins, P.J. and Cooney, R.T., 2005. Digital Geology Map of British Columbia, Open File 2005-2, DVD. B.C.M.o.E.a. Mines.

Mathews, W.H., 1989. Neogene Chilcotin basalts in south-central British Columbia: geology, ages, and geomorphic history. Canadian Journal of Earth Sciences 26, 969–982.

McClaughry, J.D., Gaylord, D.R., 2005. Middle Eocene sedimentary and volcanic infilling of an evolving supradetachment basin: White Lake Basin, south-central British Columbia. Canadian Journal of Earth Sciences 42 (1), 49–66.

McKervey, J.A., 1998. The petrogenesis of the Eocene Challis Volcanic Group, Idaho, western United States. PhD Thesis, Open University, Milton Keynes, 586 pp.

McMechan, R.D., 1983. Geology of the Princeton Basin. British Columbia. Ministry of Energy, Mines and Petroleum Resources; Paper 1983-3. British Columbia Ministry of Energy, Mines and Petroleum Resources, Victoria. 52 pp.

Melcher, F., Meisel, T., 2004. A metamorphosed early Cambrian crust–mantle transition in the Eastern Alps, Austria. Journal of Petrology 45 (8), 1689–1723.

Miyashiro, A., 1974. Volcanic rock series in island arcs and active continental margins. American Journal of Science 274 (4), 321–355.

Monger, J., 1985. Structural evolution of the southwestern Intermontane belt, Ashcroft and Hope map areas, British Columbia. Current Research, Part A, Paper 85-1A, pp. 349–358.

Monger, J., 1989. Geology, Hope, British Columbia. Geological Survey of Canada.

Monger, J., McMillan, W.J., 1989. Geology, Ashcroft, British Columbia. Geological Survey of Canada.

Monger, J., Price, R.A., 2002. The Canadian Cordillera: geology and tectonic evolution. CSEG Recorder 27, 17–36.

Morris, G.A., Creaser, R.A., 2003. Crustal recycling during subduction at the Eocene Cordilleran margin of North America: a petrogenetic study from the southwestern Yukon. Canadian Journal of Earth Sciences 40 (12), 1805–1821.

Morris, G.A., Hooper, P.R., 1997. Petrogenesis of the Colville Igneous Complex, northeast Washington: implications for Eocene tectonics in the northern US Cordillera. Geology 25 (9), 831–834.

Morris, G.A., Larson, P.B., Hooper, P.R., 2000. 'Subduction style' magmatism in a nonsubduction setting: the Colville Igneous Complex, NE Washington State, USA. Journal of Petrology 41 (1), 43–67.

Mortimer, N., 1987. The Nicola Group: Late Triassic and Early Jurassic subduction-related volcanism in British Columbia. Canadian Journal of Earth Sciences 24, 2521–2536.

Norman, M.D., Mertzman, S.A., 1991. Petrogenesis of Challis volcanics from central and southwestern Idaho-Trace-element and Pb isotopic evidence. Journal of Geophysical Research-Solid Earth and Planets 96 (B8), 13279–13293.

Parrish, R.R., Carr, S.D., Parkinson, D.L., 1988. Eocene extensional tectonics and geochronology of the southern Omineca Belt, British-Columbia and Washington. Tectonics 7 (2), 181–212.

Peacock, M.A., 1931. Classification of igneous rock series. Journal of Geology 39, 54–67.

Pearce, J.A., Peate, D.W., 1995. Tectonic implications of the composition of volcanic arc magmas. Annual Review of Earth and Planetary Sciences 23, 251–285.

Peslier, A.H., Reisberg, L., Ludden, J., Francis, D., 2000. Os isotopic systematics in mantle xenoliths; age constraints on the Canadian Cordillera lithosphere. Chemical Geology 166 (1–2), 85–101.

Rapp, R.P., 1995. Amphibole-out phase-boundary in partially melted metabasalt, its control over liquid fraction and composition, and source permeability. Journal of Geophysical Research-Solid Earth 100 (B8), 15601–15610.

Rapp, R.P., Watson, E.B., 1995. Dehydration melting of metabasalt at 8–32-Kbar — Implications for continental growth and crust–mantle recycling. Journal of Petrology 36 (4), 891–931.

Rapp, R.P., Watson, E.B., Miller, C.F., 1991. Partial melting of amphibolite eclogite and the origin of Archean trondhjemites and tonalites. Precambrian Research 51 (1–4), 1–25.

Rapp, R.P., Shimizu, N., Norman, M.D., Applegate, G.S., 1999. Reaction between slab-derived melts and peridotite in the mantle wedge: experimental constraints at 3.8 GPa. Chemical Geology 160 (4), 335–356.

Read, P.B., 2000. Geology and Industrial Minerals of the Tertiary Basins, South-central British Columbia. British Columbia. Ministry of Energy, Mines and Petroleum Resources Geofile 2000-3. British Columbia. Ministry of Energy, Mines and Petroleum Resources, Victoria, 110 pp.

Rice, H.M.A., 1947. Geology and mineral deposits of the Princeton map-area, British Columbia. Geological Survey of Canada, Memoir, vol. 243. Geological Survey of Canada. 136 pp.

Riedel, C., Ernst, G.G.J., Riley, M., 2003. Controls on the growth and geometry of pyroclastic constructs. Journal of Volcanology and Geothermal Research 127 (1–2), 121–152.

Roeder, P., Emslie, R., 1970. Olivine-liquid equilibrium. Contributions to Mineralogy and Petrology 29, 275–289.

Rudnick, R.L., Gao, S., 2003. Composition of the continental crust. In: Rudnick, R.L. (Ed.), The Crust. Treatise on Geochemistry. Elsevier, pp. 1–64.

Rushmer, T., 1991. Partial melting of 2 amphibolites — contrasting experimental results under fluid-absent conditions. Contributions to Mineralogy and Petrology 107 (1), 41–59.

Sen, C., Dunn, T., 1994. Dehydration melting of a basaltic composition amphibolite at 1.5 and 2.0 GPa — implications for the origin of adakites. Contributions to Mineralogy and Petrology 117 (4), 394–409.

Shaw, W.S., 1952. The Princeton Coalfield, B.C. Paper 52-12. Geological Survey of Canada.

Sisson, V.B., Pavlis, T.L., Roeske, S.M., Thorkelson, D.J., 2003. Introduction: an overview of ridge-trench interactions in modern and ancient settings. In: Sisson, V.B., Roeske, S.M., Pavlis, T.L. (Eds.), Special Paper 371: Geology of a Transpressional Orogen Developed During Ridge-Trench Interaction Along the North Pacific Margin. Geological Society of America, Boulder, CO, pp. 1–18.

Smith, A.D., Thorkelson, D., 2002. Geochemical and Nd–Sr–Pb isotopic evidence on the origin and geodynamic evolution of mid-Cretaceous continental arc volcanic rocks of the Spences Bridge Group, south-central British Columbia. Geological Journal 37 (2), 167–186.

Souther, J.G., 1991. Volcanic regimes. In: Gabrielse, H., Yorath, C.J. (Eds.), Geology of the Cordilleran Orogen in Canada. Geology of Canada. Geological Survey of Canada, pp. 457–490.

Stern, C.R., Kilian, R., 1996. Role of the subducted slab, mantle wedge and continental crust in the generation of adakites from the Andean Austral volcanic zone. Contributions to Mineralogy and Petrology 123 (3), 263–281.

Streck, M.J., Leeman, W.P., Chesley, J., 2007. High-magnesian andesite from Mount Shasta: a product of magma mixing and contamination, not a primitive mantle melt. Geology 35 (4), 351–354.

Sun, S.S., McDonough, W.F., 1989. Chemical and isotopic systematics of oceanic basalts: implications for mantle composition and process. In: Saunders, A.D., Norry, M.J. (Eds.), Magmatism in the Ocean Basins. The Geological Society, pp. 313–345.

Thorkelson, D.J., 1989. Eocene sedimentation and volcanism in the Fig Lake Graben, southwestern British-Columbia. Canadian Journal of Earth Sciences 26 (7), 1368–1373.

Thorkelson, D.J., 1996. Subduction of diverging plates and the principles of slab window formation. Tectonophysics 255 (1–2), 47–63.

Thorkelson, D.J., Breitsprecher, K., 2005. Partial melting of slab window margins: genesis of adakitic and non-adakitic magmas. Lithos 79 (1–2), 25–41.

Thorkelson, D.J., Taylor, R.P., 1989. Cordilleran slab windows. Geology 17 (9), 833–836.

Valentine, G.A., Krier, D., Perry, F.V., Heiken, G., 2005. Scoria cone construction mechanisms, Lathorp Wells volcano, southern Nevada, USA. Geology 33 (8), 629–632.

Vielzeuf, D., Schmidt, M.W., 2001. Melting relations in hydrous systems revisited: application to metapelites, metagreywackes and metabasalts. Contributions to Mineralogy and Petrology 141 (3), 251–267.

Villeneuve, M.E., Mathewes, R.W., 2005. An Early Eocene age for the Quilchena fossil locality, southern British Columbia. Geological Survey of Canada, Current Research A4, 1–7.

von Huene, R., Ranero, C.R., Vannucchi, P., 2004. Generic model of subduction erosion. Geology 32 (10), 913–916.

Weis, D., Kieffer, B., Maerschalk, C., Pretorius, W., Barling, J., 2005. High-precision Pb–Sr–Nd–Hf isotopic characterization of USGS BHVO-1 and BHVO-2 reference materials. Geochemistry Geophysics Geosystems 6.

Wheeler, J.O. and McFeeley, P., 1991. Tectonic assemblage map of the Canadian Cordillera and adjacent parts of the United States of America. Map 1712A. Geological Survey of Canada.

Williams, V.E., Ross, C.A., 1979. Depositional setting and coal petrology of Tulameen Coalfield, south-central British-Columbia. AAPG Bulletin-American Association of Petroleum Geologists 63 (11), 2058–2069.

Wolf, M.B., Wyllie, P.J., 1994. Dehydration-melting of amphibolite at 10 Kbar — the effects of temperature and time. Contributions to Mineralogy and Petrology 115 (4), 369–383.

Wood, B.J., Blundy, J.D., 2003. Trace element partitioning under crustal and uppermost mantle conditions: the influence of ionic radius, cation charge, pressure, and temperature. In: Rudnick, R.L. (Ed.), The Crust. Treatise on Geochemistry. Elsevier, pp. 395–424.

Xiong, X.L., Adam, J., Green, T.H., 2005. Rutile stability and rutile/melt HFSE partitioning during partial melting of hydrous basalt: implications for TTG genesis. Chemical Geology 218–359 (3–4), 339.

Xu, J.F., Shinjo, R., Defant, M.J., Wang, Q.A., Rapp, R.P., 2002. Origin of Mesozoic adakitic intrusive rocks in the Ningzhen area of east China: partial melting of delaminated lower continental crust? Geology 30 (12), 1111–1114.